Supplementary methods

Cloning of *zyx-1(js417)*

sam-6(js417) was positioned roughly equidistant between *rol-1* (6.9 mu) and *lin-31* (22.9 mu) on chromosome II by two-factor mapping. Subsequently *sam-6(js417); jsIs821* animals were crossed to males of a CB4856 Hawaiian derivative that had been backcrossed 10 times into *jsIs821*. Heterozygous cross progeny were cloned and 120 F2 *sam-6* homozygote animals were cloned and analyzed by PCR with single nucleotide polymorphism (SNP) markers pkP2111 and pkP2116 at 7.5 and 16.1 mu on chromosome II. SNP markers are detailed in Table S6. In all animals homozygous at one marker and heterozygous at the other, the position of recombination events was defined by SNP analysis yielding: (*pKP2111*) 6 (haw31582) 4 (*pkP2112* Y38F1[10]) 1 (F42G4[1]) 1 (F42G4[5]) 0 (uCE2-2180) 1 (CE2-207) 1 (*pKP2116*). This positioned *js417* to a 174 kb region. Germline transformation experiments revealed that injection of the WRM0617bB03 fosmid in this interval rescued the Sam phenotype of non-Lin *sam-6(js417)*; *jsIs821 lin-15(n765)*; *jsEx968* [WRM0617bB03; WRM062bF09 (*lin-15*); pUC18 (10 ng:10 ng:150 ng) animals. Likewise, a clone containing only the genomic *zyx-1* locus (pZyx-1gen) consisting of 6 kb of promoter, the entire *zyg-1* genomic interval and 500 bp of 3' UTR of the *zyx-1* gene also rescued the Sam phenotypes of GFP positive *sam-6(js417); jsIs821; jsEx985* [NM 1798(pZyx-1gen) ;pPD118.33 (P*myo-2*::GFP); pBluescript (30 ng, 5 ng,100 ng)] animals. Sequencing of *js417* identified a G to A lesion in the splice-donor site of the first exon of the *zyx-1b* isoform (ATGGCGGATCAAGAAG[g]ttcgttttt). Lastly, *zyx-1(gk190)* failed to complement *js417* for Sam phenotypes.

Plasmid constructions

Unless noted all plasmids were constructed by transformation into DH5α.

NM1798 : *pZyx-1gen*. A *zyx-1* genomic construct containing 6 kb of promoter, the entire coding region and 500 bp 3' UTR region. *zyx-1* genomic sequences were gap repaired into the NM1019 plasmid vector backbone (Mahoney et al., 2006) using a fosmid recombineering approach (Sarov et al., 2006). The vector was PCR amplified using oligonucleotides 3184 and 3185 and electroporated into EC1300 cells containing the *zyx-1* fosmid 17bB03 followed by selection for ampicillin resistance.

NM1849 *pR6KanRmCherry*. A mCherry version of the R6K origin plasmid pR6KGFP with the FRT Kan^R cassette 5' of mCherry to create C-terminal mCherry fusions using recombineering (Sarov et al., 2006). The mCherry gene (from UAS::M-mcherry (Godinho et al., 2005), the Kan^R cassette (from pR6KGFP) and the R6K Amp vector (from pR6KGFP) were independently amplified using the oligonucleotides 3272 and 3273, 3266 and 3271, and 3265 and 3274, respectively. The resulting fragments were co-assembled by mixing the products and performing an additional PCR amplification using oligonucleotides 3265 and 3266. The resulting PCR product was digested with EcoRI, ligated and transformed into DH5α λpir^+ strain with selection for ampicillin and kanamycin resistance.

NM1860: *pmcherry::zyx-1*. A *zyx-1* genomic construct with *mCherry* fused at the N-terminus created using a recombineering pipeline protocol (Sarov et al., 2006). Briefly, a 1.8kb Kan^R mCherry fragment was amplified from the plasmid NM1849 pR6KKanRmcherry using oligonucleotides 3275 and 3277, digested with DpnI to remove

the template plasmid, and electroporated into EC1300 cells containing the *zyx-1* fosmid 17bB03 followed by selection for kanamycin. After recombination, the Kan^R cassette was removed by anhydrotetracycline treatment (Sarov et al., 2006), and the *mCherry::zyx-1* fragment was gap repaired into the NM1019 vector backbone as described for NM1798.

NM1874: *pzyx-1::GFP.* A *zyx-1* genomic construct with *GFP* fused at the C-terminus created using a recombineering pipeline protocol (Sarov et al., 2006). Briefly, a 1.8kb GFPKanR fragment was amplified from the plasmid pR6KGFP (Sarov et al., 2006) using oligonucleotides 3278 and 3279. The PCR product was digested with DpnI to remove the template plasmid, electroporated into cells containing *zyx-1* 17bB03. After recombination, the Kan^R was removed by anhydrotetracycline treatment, and the *zyx-1::GFP* fragment was gap repaired into the NM1019 vector backbone as described for NM1798.

NM1934: *Pmec-7::zyx-1::GFP.* A full-length *zyx-1* cDNA with *GFP* fused at the C-terminus expressed under the *mec-7* promoter. The full-length *zyx-1* cDNA was amplified from the cDNA clone yk1054c06 (Yuji Kohara, unpublished EST cDNA in Wormbase) using oligonucleotides 3362 and 3263, digested with BamHI and KpnI and inserted into similarly digested pPD117.01 (Fire Lab 1997 vector kit).

NM1938: *Pglr-1::zyx-1::GFP.* A full-length *zyx-1* cDNA with *GFP* fused at the C-terminus expressed under the *glr-1* promoter. The full-length *zyx-1* cDNA was amplified from the cDNA clone yk1054c6 using oligonucleotides 3362 and 3364, digested with BamHI and SpeI, and inserted into similarly digested NM1707 *glr-1$_p$::aex-2::GFP* (Mahoney et al., 2008) replacing *aex-2* with *zyx-1*.

NM1941: *Pmyo-3::zyx-1::YFP.* A full-length *zyx-1* cDNA with *YFP* fused at the C-terminus expressed under the muscle specific *myo-3* promoter. The *zyx-1* full-length cDNA was amplified from the cDNA clone yk1054c6 using oligonucleotides 3365 and 3366, digested with NheI and StuI and inserted into similarly digested NM2102 *myo-3$_p$::aex-2::yfp* (Mahoney et al., 2008) replacing *aex-2* with *zyx-1*.

NM2002: *Pmec-7::GFP::zyx-1(1-427).* A cDNA fragment encoding ZYX-1A a.a. 1-427 was fused with *GFP* at the N-terminus under the *mec-7* promoter. *GFP* was PCR amplified from pPD117.01 using oligonucleotides 3406 and 3407 and the *zyx-1* fragment was amplified from cDNA clone yk1054c6 using oligonucleotides 3608 and 3609, co-assembled by overlap PCR, digested with KpnI and EcoRV and inserted into similarly digested pPD96.41 (Fire Lab 1995 vector Kit).

NM2004: *Pmec-7::GFP::zyx-1(1-293).* A cDNA fragment encoding ZYX-1A a.a. 1-293 was fused with *GFP* at the N-terminus under the *mec-7* promoter. *GFP* was PCR amplified from pPD117.01 using oligonucleotides 3406 and 3407 and the *zyx-1* fragment was amplified from cDNA clone yk1054c6 using oligonucleotides 3608 and 3610, co-assembled by overlap PCR, digested with KpnI and EcoRV and inserted into similarly digested pPD96.41 (Fire Lab 1995 vector Kit).

NM2006: *Pmec-7::GFP::zyx-1(294-603).* A cDNA fragment encoding ZYX-1A a.a. 294-603 was fused with *GFP* at the N-terminus under the *mec-7* promoter. *GFP* was PCR amplified from pPD117.01 using oligonucleotides 3406 and 3411 and the *zyx-1* fragment was amplified from cDNA clone yk1054c6 using oligonucleotides 3612 and 3613, co-assembled by overlap PCR, digested with KpnI and EcoRV and inserted into similarly digested pPD96.41 (Fire Lab 1995 vector Kit).

NM2008: *Pmec-7::GFP::zyx-1(428-603).* A cDNA fragment encoding ZYX-1A a.a. 428-603 was fused with *GFP* at the N-terminus under the *mec-7* promoter. *GFP* was PCR amplified from pPD117.01 using oligonucleotides 3406 and 3414 and the *zyx-1* fragment was amplified from cDNA clone yk1054c6 using oligonucleotides 3615 and 3613, co-assembled by overlap PCR, digested with KpnI and EcoRV and inserted into similarly digested pPD96.41 (Fire Lab 1995 vector Kit).

NM2016: P*mec-7::mcherry::zyx-1::GFP.* A full-length *zyx-1* cDNA fused with *mCherry* at the N-terminus and *GFP* at the C-terminus under the derivative of *mec-7* promoter. *mCherry* was PCR amplified from pRSETB-mCherry (Shaner et al., 2004) using oligonucleotides 3419 and 3420 and *zyx-1* from cDNA clone yk1054c6 using oligonucleotides 3421 and 3363, co-assembled by overlap PCR, digested with BamHI and KpnI and inserted into similarly digested pPD117.01.

NM2122: P*mec-7::mcherry::zyx-1::GFP CBunc-119.* NM2016 was then digested with SphI and XbaI and inserted with SphI/XbaI fragment containing *C. briggsae unc-119* from pCBunc-119 (which contains a 2.0-kb *C. briggsae unc-119* gene fragment in pDONR221, gift of M. Driscoll, Rutgers University).

NM2387: *Pmec-7::Venus::LIM1*. A cDNA fragment encoding the LIM1 domain (a.a.406-467) fused with *Venus* at the N-terminus under the *mec-7* promoter. *Venus* was PCR amplified from NM1358 prab-3VenusRim3' which contains Venus derived from pDEST-VENUS (Matsuki et al., 2006) using oligonucleotides 3406 and 4138 and the LIM1 domain from cDNA clone yk1054c6 using oligonucleotides 4139 and 4140. The fragments were co-assembled by overlap PCR, digested with KpnI and EcoRV and inserted into similarly digested pPD96.41.

NM2389: *Pmec-7::Venus::LIM2.* A cDNA fragment encoding the LIM2 domain (a.a.468-526) fused with *Venus* at the N-terminus under the *mec-7* promoter. *Venus* was PCR amplified from NM1358 using oligonucleotides 3406 and 4141 and the LIM2 domain from cDNA clone yk1054c6 using oligonucleotides 4142 and 4143. The fragments were co-assembled by overlap PCR, digested with KpnI and EcoRV and inserted into similarly digested pPD96.41.

NM2390: *Pmec-7::Venus::LIM3*. A cDNA fragment encoding the LIM3 domain (a.a.527-603) fused with *Venus* at the N-terminus under the *mec-7* promoter. *Venus* was PCR amplified from NM1358 using oligonucleotides 3406 and 4144 and the LIM3 domain from cDNA clone yk1054c6 using oligonucleotides 4145 and 3413. The fragments were co-assembled by overlap PCR, digested with KpnI and EcoRV and inserted into similarly digested pPD96.41.

NM2391: *Pmec-7::Venus::LIM1,2*. A cDNA fragment encoding the LIM1 and LIM2 domains (a.a. 406-526) fused with *Venus* at the N-terminus under the *mec-7* promoter. *Venus* was PCR amplified from NM1358 using oligonucleotides 3406 and 4138 and the LIM1 and LIM2 domains from cDNA clone yk1054c6 using oligonucleotides 4139 and 4143. The fragments were co-assembled by overlap PCR, digested with KpnI and EcoRV and inserted into similarly digested pPD96.41.

NM2392: *Pmec-7::Venus::LIM2,3*. A cDNA fragment encoding the LIM2 and LIM3 domains (a.a. 468-603) fused with *Venus* at the N-terminus under the *mec-7* promoter. *Venus* was PCR amplified from NM1358 using oligonucleotides 3406 and 4141 and the LIM2 and LIM3 domains from cDNA clone yk1054c6 using

oligonucleotides 4142 and 3413. The fragments were co-assembled by overlap PCR, digested with KpnI and EcoRV and inserted into similarly digested pPD96.41.

NM2394: *Pmec-7::Venus::LIM1,3*. cDNA fragments encoding the LIM1 and LIM3 domains (a.a.406-467, 527-603) fused with *Venus* at the N-terminus under the *mec-7* promoter. *Venus* was PCR amplified from NM1358 using oligonucleotides 3406 and 4138, the LIM1 from cDNA clone yk1054c6 using oligonucleotides 4139 and 3413 and the LIM3 domain from cDNA clone yk1054c6 using oligonucleotides 4147 and 3413. The fragments were co-assembled by overlap PCR, digested with KpnI and EcoRV and inserted into similarly digested pPD96.41.

NM2395: *P1zyx-1::nlsYFP*. Nuclear localized YFP driven by the *zyx-1A* P1 promoter and the first intron. Nuclear localized *YFP* was PCR amplified from PJL43-nlsYFP which contains an *nlsYFP* from the plasmid pPD132.112 (Fire lab 1999 Vector Kit) using oligonucleotides 4128 and 4129 and the *zyx-1*A promoter and first exon was amplified from NM1798 using oligonucleotides 4126 and 4127. The two fragments were co-assembled by overlap PCR, digested with NheI and XhoI, and inserted into a similarly digested vector backbone PCR amplified from NM1019 using oligonucleotides 4130 and 4131.

NM2397: *P3zyx-1::nlsYFP*. Nuclear localized YFP driven by the *zyx-1D* P3 promoter located in the fifth intron. Nuclear localized *YFP* was PCR amplified from PJL43-nlsYFP using oligonucleotides 4134 and 4129 and the *zyx-1D* promoter was amplified from NM1798 using oligonucleotides 4132 and 4133. The two fragments were co-assembled by overlap PCR, digested with NheI and XhoI, and inserted into a similarly

digested vector backbone PCR amplified from NM1019 using oligonucleotides 4130 and 4131.

NM2399: *P4zyx-1::nlsYFP*. Nuclear localized YFP driven by the *zyx-1B* promoter located in the sixth intron. Nuclear localized *YFP* was PCR amplified from PJL43-nlsYFP using oligonucleotides 4137 and 4129 and the *zyx-1* sixth intron P4 promoter was amplified from NM1798 using oligonucleotides 4135 and 4136. The two fragments were co-assembled by overlap PCR, digested with NheI and XhoI, and inserted into a similarly digested vector backbone PCR amplified from NM1019 using oligonucleotides 4130 and 4131.

NM2909: Δ*P1-3zyx-1b*. A genomic clone with the P1 and P2 promoters deleted. NM1798 was digested with NheI and re-ligated to delete 9 kb of promoter and first intron sequences.

NM2911: *Pmec-7::GFP::zyx-1b*. NM2006 was modified using a megaprimer and DpnI-mediated site-directed mutagenesis (Tseng et al., 2008) using oligonucleotides 3384 and 4852. This resulted in the removal of sequences coding for a.a. 294-409 of ZYX-1A, the addition of sequences coding for a.a. 1-6 from ZYX-1B to create a complete GFP::ZYX-1B cDNA fusion under the *mec-7* promoter.

NM2918: Δ*P1-3zyx-1b::GFP*. NM1874 was digested with NheI and NruI, filled in with dNTPs using T4 DNA polymerase and re-ligated to remove a 13.8 kb region including the P1 and P2 promoters from the genomic *zyx-1::GFP* clone.

NM3099 and NM 3100: *eGFP::zyx-1B*. An *eGFP::zyx-1B* genomic construct that encodes the translational fusion of eGFP at the N-terminus of ZYX-1B generated using recombineering (Sarov *et al.*, 2006). Briefly, *eGFP* sequences were amplified from

the plasmid NM1847 pR6KKanRGFP using the oligonucleotides 5157 and 5218. The PCR product was digested with DpnI to remove template DNA, gel purified and 1µl of the purified product was electroporated into the L-rhamnose-induced competent bacterial cells that harbor the helper plasmid pREDFlp4 (NM1834) and the fosmid containing full-length *zyx-1* genomic DNA. Successful recombinants with e*GFP* recombined into the *zyx-1* fosmid were selected by kanamycin resistance, with the *kan*^{r} gene subsequently removed by anhydrotetracycline-induced Flp recombination. Two *zyx-1* containing fosmids, 26cB12 (NM3099) and 31aG09 (NM3100), were used to generate *eGFP::zyx-1B* fusion constructs. The correct insertion of *eGFP* upstream of *zyx-1b* was verified by sequencing.

Analysis of neuronal morphology of other cell types and PLM neurons expressing other markers

Images of animals expressing fluorescent proteins in PVD, GABAergic, cholinergic or GLR-1 expressing neurons were mounted at described above and imaged using either an Olympus 500a confocal microscope, a Zeiss fluorescent image LSM500 microscope, or on a compound microscope described above. Images were subsequently processed in Adobe Photoshop. For the time-course imaging of wild-type and *zyx-1* animals expressing mRFP, mito::GFP or UNC-10::GFP (or combinations of these markers), the eggs of appropriate fluorescent lines were collected and allowed to hatch at RT, and groups of about 20 L1 larvae were picked at various time points after hatching for analysis. Images were acquired as described for quantification of PLM development.

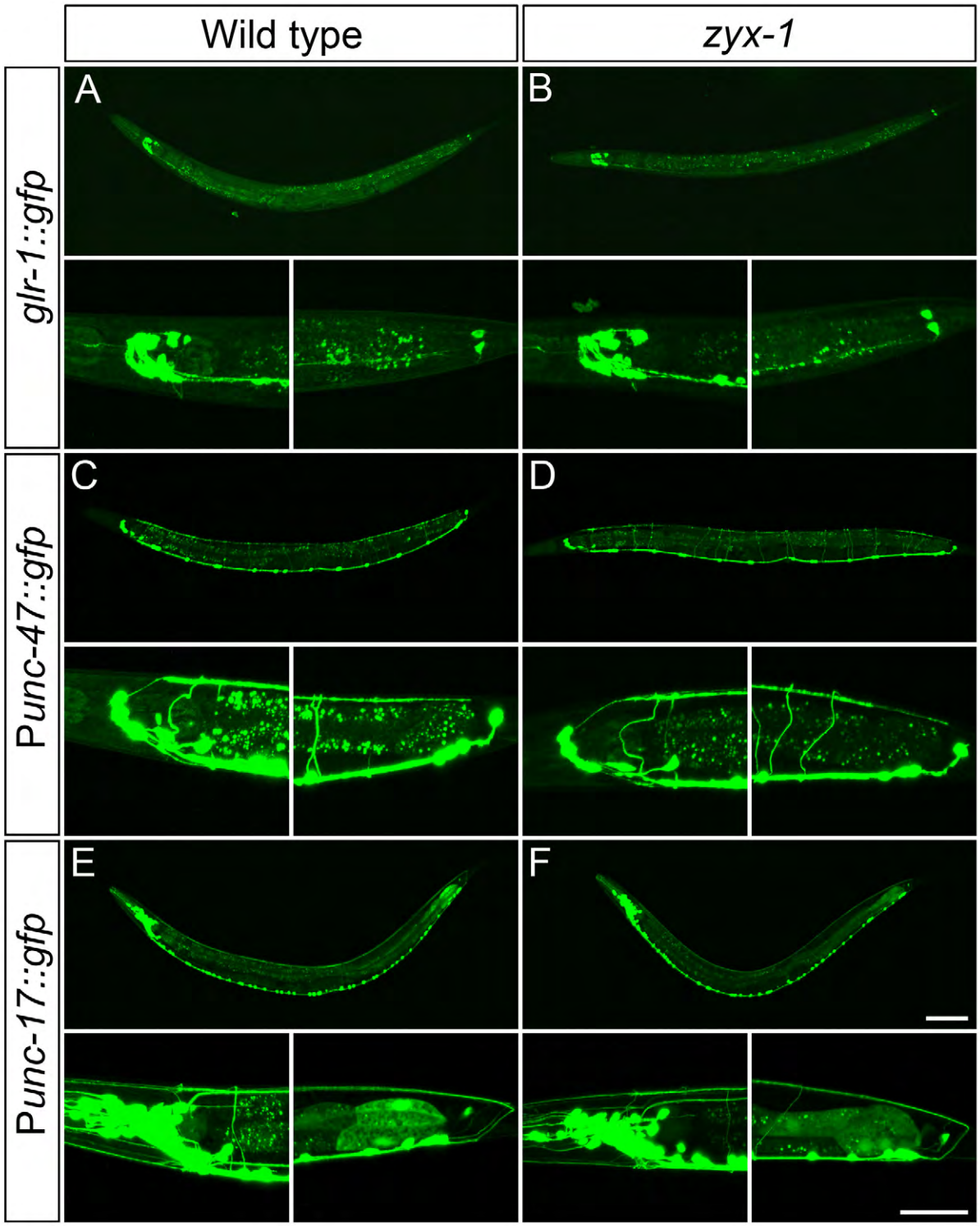

Figure S1. ***zyx-1*** **mutants have normal structures in cholinergic, GABAergic, and GLR-1-positive interneuronal systems**
Confocal images of *zyx-1(gk190)* mutants carrying integrated transgenic lines *nuIs25* that stably expresses GFP in GLR-1-positive command interneurons (A, B), *oxIs12* that stably expresses GFP in GABAergic neurons (C, D), and *mdIs135* that stably expresses GFP in cholinergic neurons (E, F) under the control of the *glr-1*, *unc-47*, and *unc-17* promoters, respectively. GABAergic commissures present in *zyx-1* (17.45 +/- 0.65 n=35) and wild -type (17.66, +/- 0.67 n=29) were comparable. Scale bars, 100 mm for whole worm views and 40 mm for enlarged views.

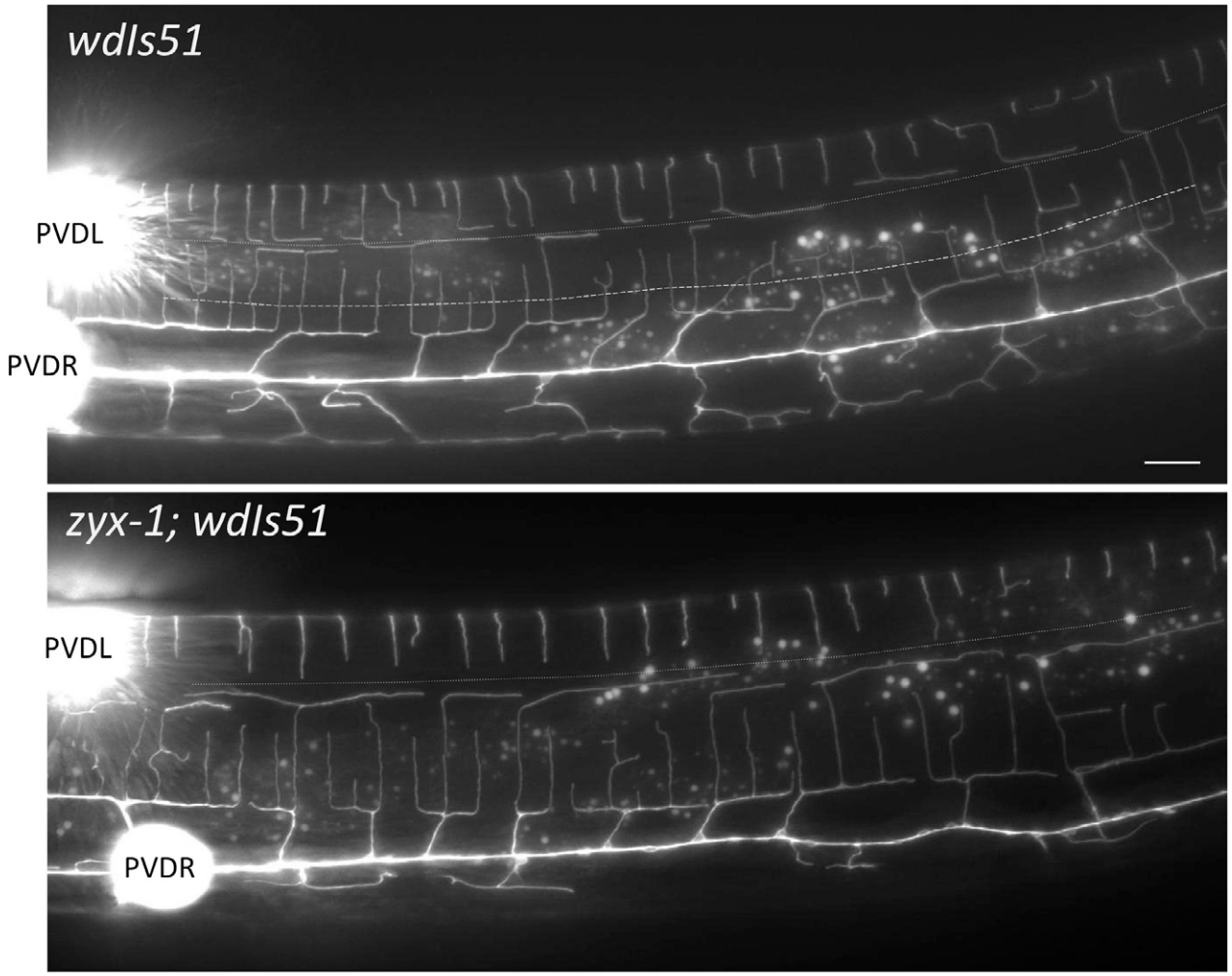

Figure S2. Morphology of PVD neurons in *zyx-1* and wildtype animals
Shown are the maximal projections of approximately 20 images taken at 0.4 µm steps showing animals from a dorsolateral view. PVDR (cell body labeled) dorsally projecting dendrites were visible, and the distal ends of PVDL (cell body labeled) dorsal dendritic projections were visible above the most dorsal position in the animal (marked by a dashed line). PVD cell bodies appeared larger than normal because of the exposure length required to detect the fine dendritic processes labeled with cytosolic GFP. Density of 4° branches was measured by counting the branches that crossed a ~200 µm length line starting just anterior of the PVD cell body and positioned parallel to and 5 µm dorsal of the 3° branches (dashed line in the *wdIs51* image). Density of 4° branches was 1 per 6.56 ± 0.83 for *wdIs51* animals (n=26 PVD neurons) and 1 per 6.79 ± 0.86 um for *zyx-1 wdIs51* double mutants (n=28 PVD neurons). Density was calculated as the length of line/(crosses-1) and errors represent ± S.D. Scale bar: 10 µm.

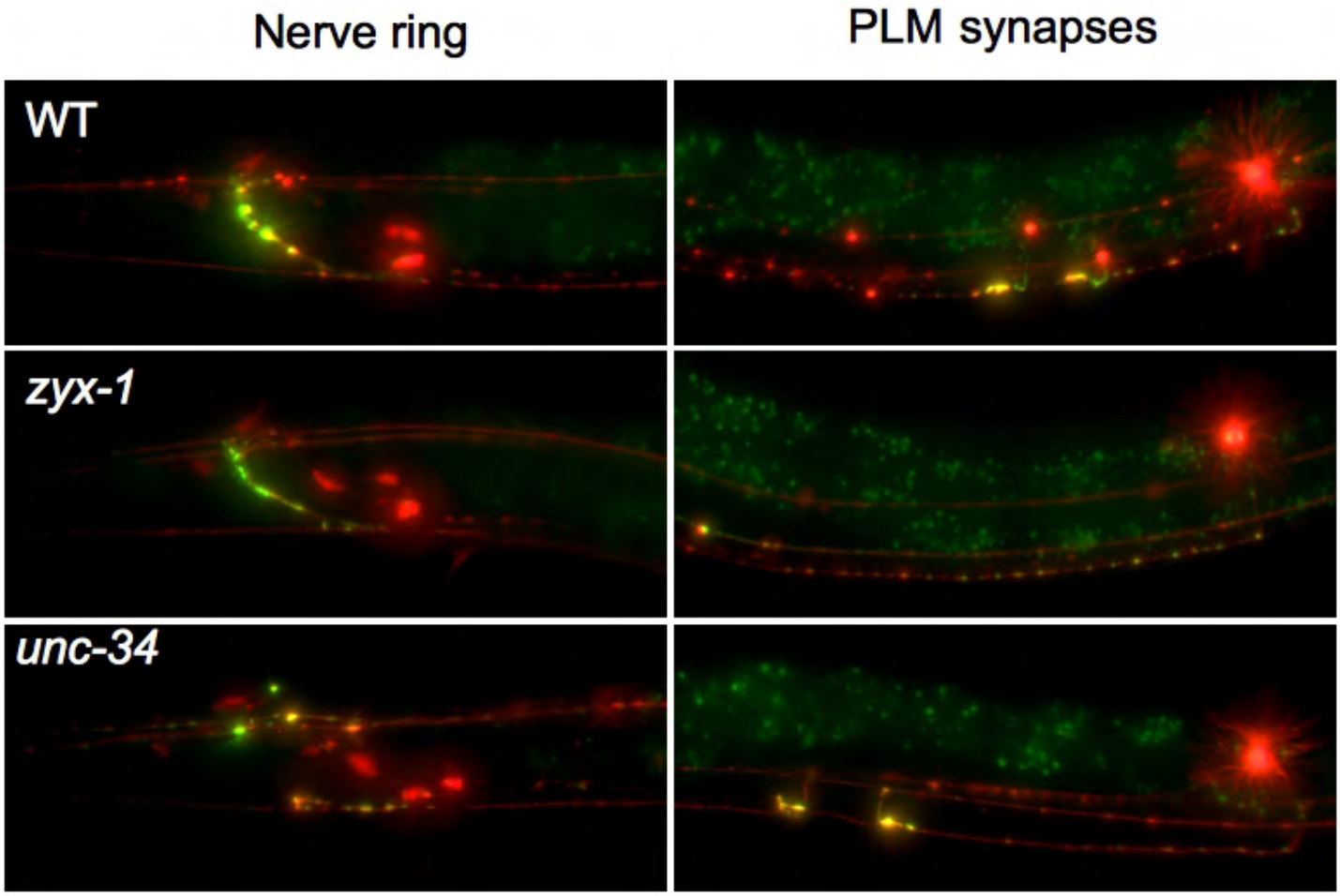

Figure S3. ***unc-34*** **but not** ***zyx-1*** **mutants fail to form ALM presynaptic varicosities in the nerve ring**
A) Images of *jsIs973*; *jsIs821* wildtype animals showing ALM presynaptic varicosities in the nerve ring (left) and PLM synaptic varicosities in the ventral cord (right).
B) Images of *zyx-1*; *jsIs973; jsIs821* animals illustrating typical wild-type ALM presynaptic varicosities in the nerve ring and defective PLM synaptic varicosities in the ventral nerve cord (right).
C) Images of *unc-34; jsIs973; jsIs821* animals illustrating the typical defects in ALM presynaptic varicosity formation in the nerve ring and wild-0type PLM synaptic varicosity formation in the ventral nerve cord.

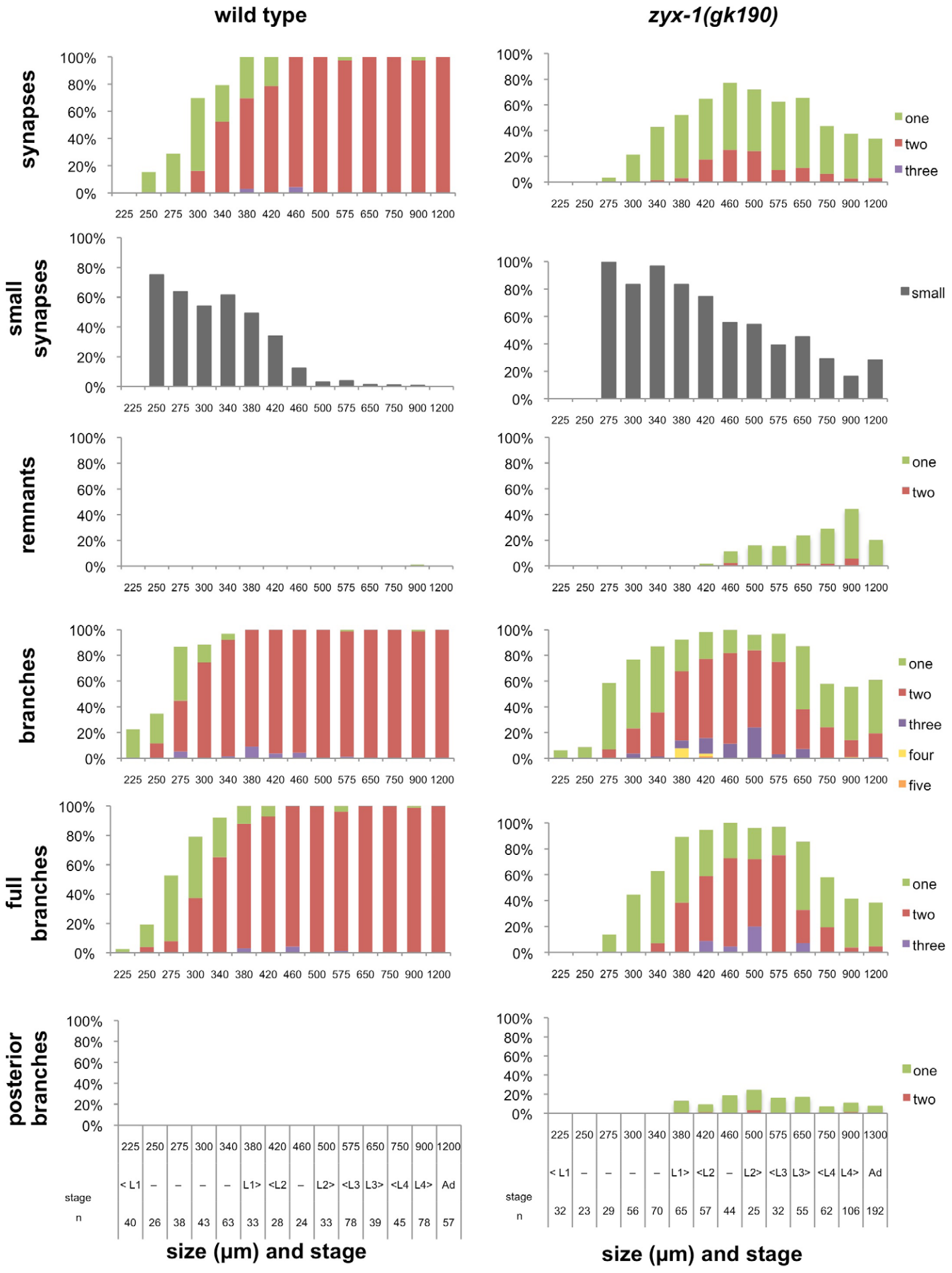
wild type
zyx-1(gk190)
synapses
small synapses
remnants
branches
full branches
posterior branches
100%
80%
60%
40%
20%
0%
225 250 275 300 340 380 420 460 500 575 650 750 900 1200
one
two
three
four
five
small
stage
n
< L1 – – – – L1> <L2 – L2> <L3 L3> <L4 L4> Ad
40 26 38 43 63 33 28 24 33 78 39 45 78 57
< L1 – – – – L1> <L2 – L2> <L3 L3> <L4 L4> Ad
32 23 29 56 70 65 57 44 25 32 55 62 106 192
size (µm) and stage
size (µm) and stage

Figure S4. Developmental timeline of wt and *zyx-1* PLM development
The fraction of animals with PLM neurons with distinct structures as a function of size is displayed in stacked columns. On the X axis each column represents animals with body sizes both less than or equal to the size (µm) listed in their own column and greater than the size specified by the prior column (or > 0 for first column). In the bottom graph the developmental larval stage correlating with each size is shown. Sample size (n= animals examined) for each column is shown in the bottom graph and this applies to all graphs of wt and *zyx-1* animals. The percentage of animals with synapses, the fraction of synapses small in size, the percentage of animals with remnants, the percentage of animals with branches, full branches, and posteriorly localized branches are all displayed. See Materials and Methods for the definition of terms.

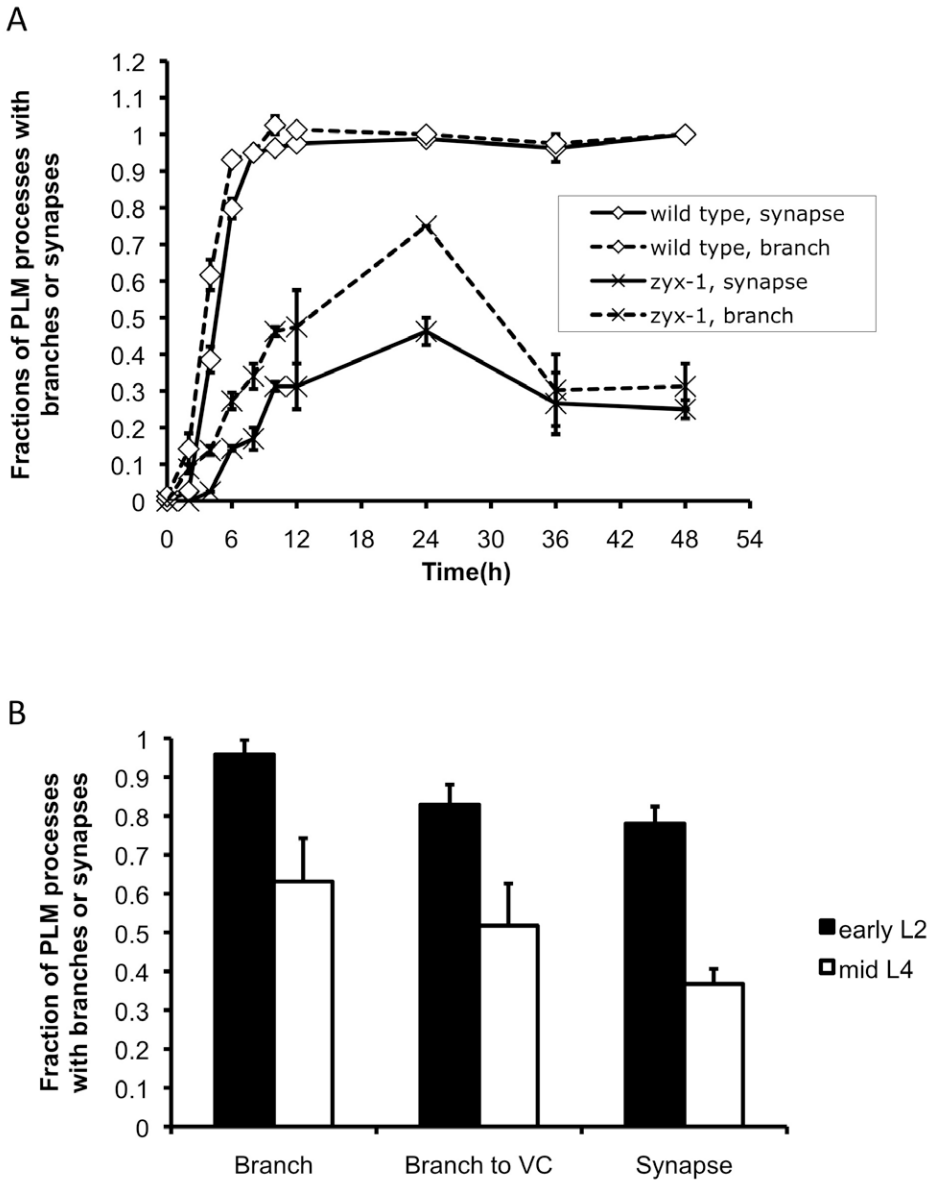

Figure S5. Development of PLM synapses in *zyx-1* animals
A) Compilation of two experiments in which groups of *wt* and *zyx-1* animals were grown at room temperature for varying numbers of hours after hatching and scored for the presence of PLM synaptic branches and PLM synaptic GFP-RAB-3 accumulations in the ventral nerve cord. Twenty animals were scored at each time point in each experiment. GFP-RAB-3 accumulations at the end of PLM processes that were larger than averagesized accumulations in PLM or PVM processes were defined as synapses. Errors represent ± S.E.M.
B) Compilation of three experiments in which groups of 20 *zyx-1* animals were anesthetized with sodium azide at the L1/L2 larval transition, scored for the presence of branches, full branches entering the VNC, and GFP-RAB-3 accumulations in the VNC. The animals were then rescued and re-anesthetized 24 hrs later in the L4 larval stage and rescored. Fifteen, eighteen, and twenty of the twenty animals were successfully rescued and rescored in the three experiments. Plotted is the fraction of PLM processes containing branches, full branches, and synapses at each time point scored. Growth was performed at 22°C. Errors represent ± S.E.M.

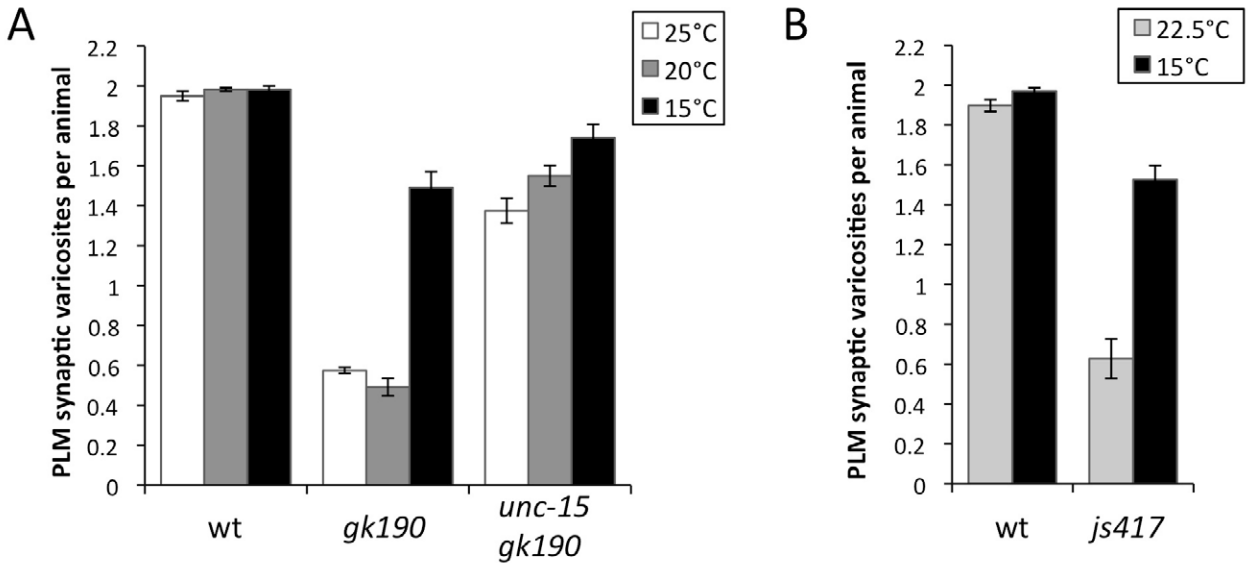

Figure S6. PLM synapse formation is temperature sensitive in *zyx-1* mutants
A) Locomotory behavior of wild-type and *zyx-1(gk190)* animals at various temperatures. B) PLM synaptic varicosities in wild-type and *zyx-1(gk190)* mutants at various temperatures.
C) PLM synaptic varicosities in wild-type and *zyx-1(js417)* animals analyzed in a *jsIs37 mec-7p-snb-1:GFP* genetic background.

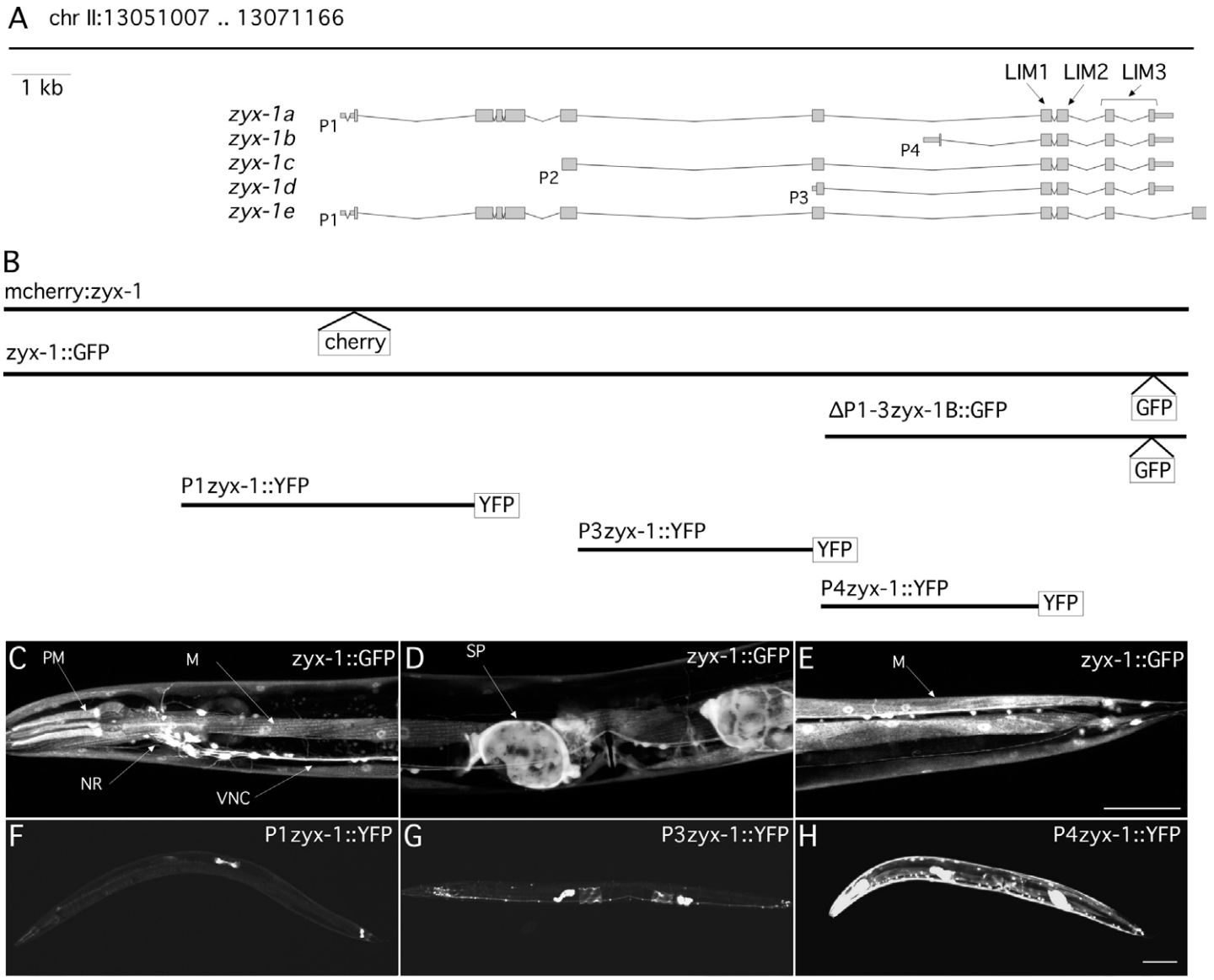

Figure S7. ***zyx-1*** **encodes a conserved LIM-domain protein widely expressed in neural and non-neural tissues.** A) Gene structure of *zyx-1*. Tall grey boxes represent coding and small grey boxes represent non-coding portions of each message. Fine lines represent splicing. Promoters are marked P1 through P4. The exons encoding the 3 conserved LIM domains are marked. B) Name and structure of the DNA constructs used to examine the expression and localization of *zyx-1* isoforms. C-E) Expression pattern of N- and C-terminal-tagged *zyx-1* constructs. *zyx-1::GFP* genomic construct exhibited wide expression in the nervous system and muscles in the head region (C), mid-body (D) and tail (E). M, muscle; PM, pharyngeal muscle, NR, nerve ring; VNC, ventral nerve cord; SP, spermatheca. Scale bar, 40 mm. F) *zyx-1* P1 promoter drove weak reporter expression in pharyngeal, body wall, enteric, and uterine muscles, and selected neurons, including tail phasmid neurons. G) The P3 promoter drove strong reporter expression in the nervous system, spermatheca and in the uterus. H) The P4 promoter and associated intron drove strong reporter expression in body wall, pharyngeal and uterine muscles, neurons and the spermatheca. Scale bar 100 mm.

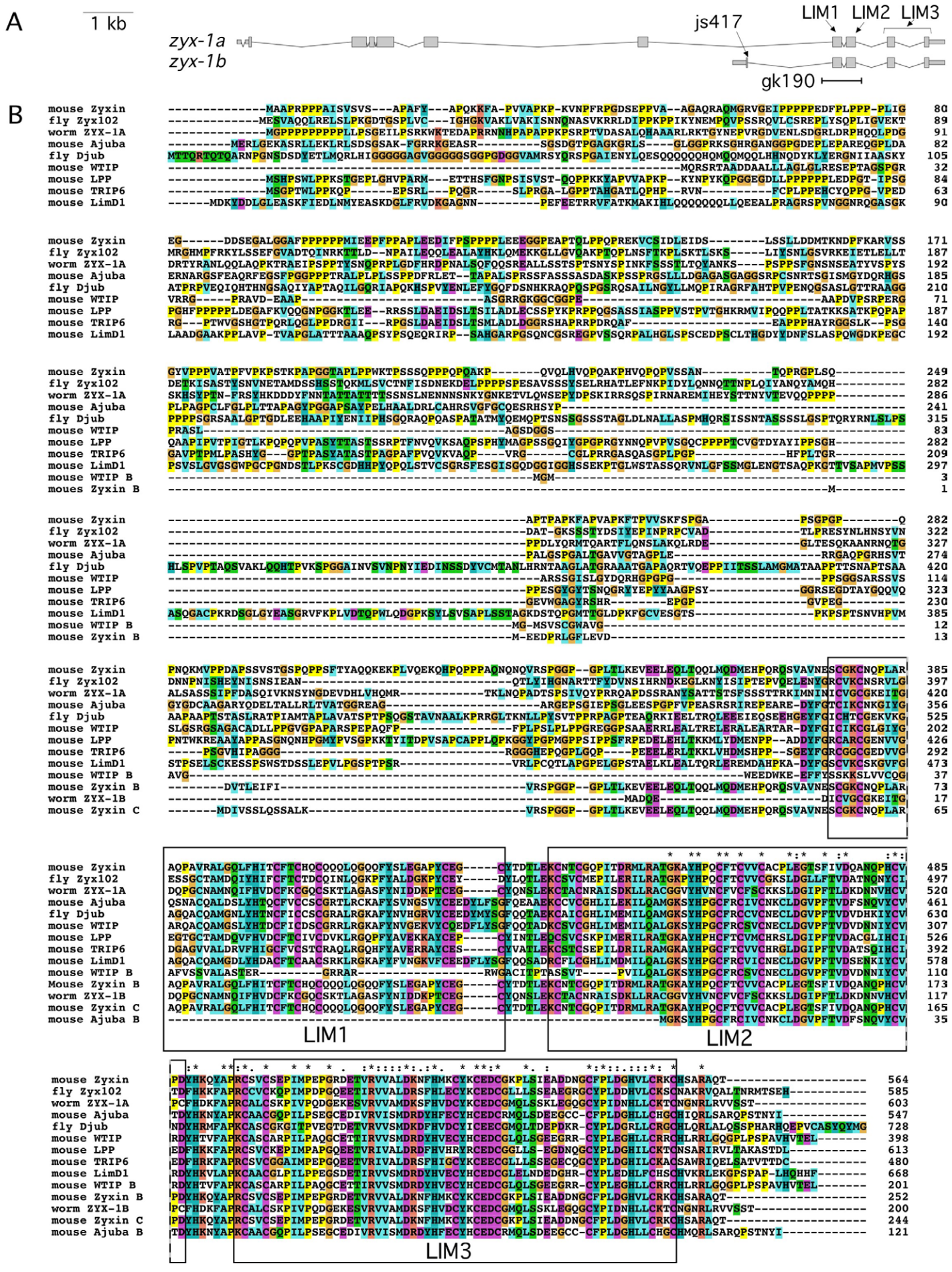
A
1 kb
zyx-1a
zyx-1b
js417
LIM1
LIM2
LIM3
gk190
B
mouse Zyxin
fly Zyx102
worm ZYX-1A
mouse Ajuba
fly Djub
mouse WTIP
mouse LPP
mouse TRIP6
mouse LimD1
mouse WTIP B
moues Zyxin B
mosue WTIP B
mouse Zyxin B
worm ZYX-1B
mouse Zyxin C
mouse Ajuba B
LIM1
LIM2
LIM3

Figure S8. *zyx-1* gene structure and protein alignments of zyxin family members

A) Structure of the *zyx-1a* and *zyx-1b* transcripts. Also shown are the positions of the *js417* and *gk190* lesions as well as the location of the three LIM domains.

B) Protein sequence alignments among *C. elegans* ZYX-1, fly zyx102, fly Djub, and mouse zyxin, Ajuba, WTIP, LPP, TRIP6 and LIMD1. Alternative smaller mouse zyxin (genbank accession BY350718 and BY783068), WTIP (genbank accession AA050259) and Ajuba (genbank accession AK012077) isoforms based upon the structure of rare cDNAs are presented in the alignment. The boxed regions denote C-terminal LIM domains, which are well-conserved compared with the N-terminal sequence. Standard amino acid single letter code is used. Protein alignments were created using Clustal X using default parameters (Larkin et al., 2007). Asterisks represent 100% conserved residues, colons represent 100% conserved strong amino acid substitution groups (e.g., acidic, basic, hydrophobic), and periods represent 100% conserved weaker substitution groups (e.g., alanine, threonine, or valine). Amino acid color code is derived from Clustal X. See documentation for details.

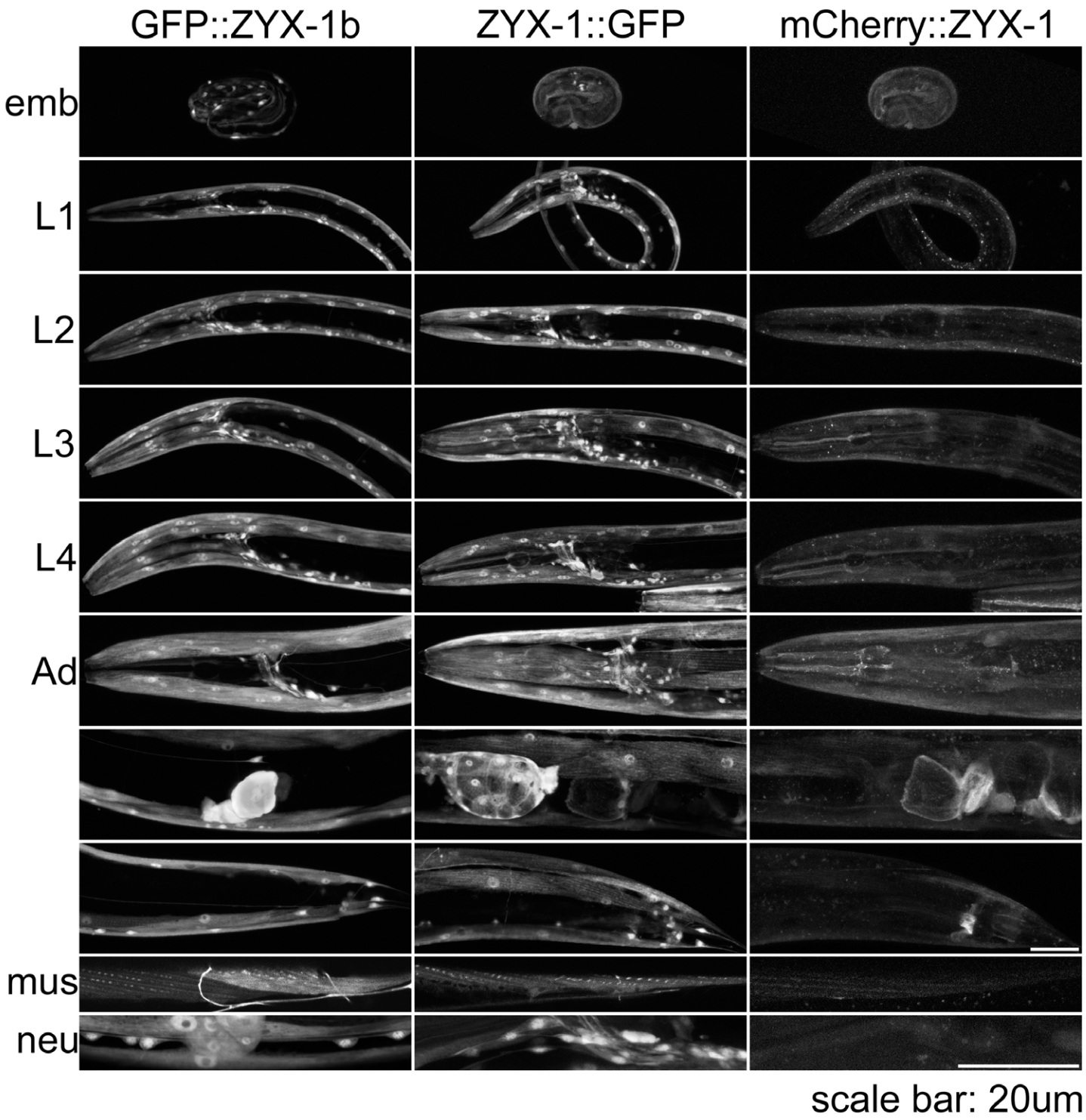

Figure S9. Developmental expression pattern of *zyx-1*
Wild-type animals carrying transgenic markers that express GFP::ZYX-1B, ZYX-1::GFP, and mCherry::ZYX-1 were imaged at various developmental stages to document the expression pattern of *zyx-1* isoforms. Representative images of 3-fold embryos, L1, L2, L3, and L4 larvae are shown. In addition, images of the Head, mid-body, and tail of adult animals are shown, along with images of both regions of body wall muscle, and ventral nerve cord neurons. Genotypes of transgenic strains used: *jsEx1388* for GFP::ZYX-1B, *jsEx1013* for ZYX-1::GFP and mCherry::ZYX-1.Scale bar 20 um.

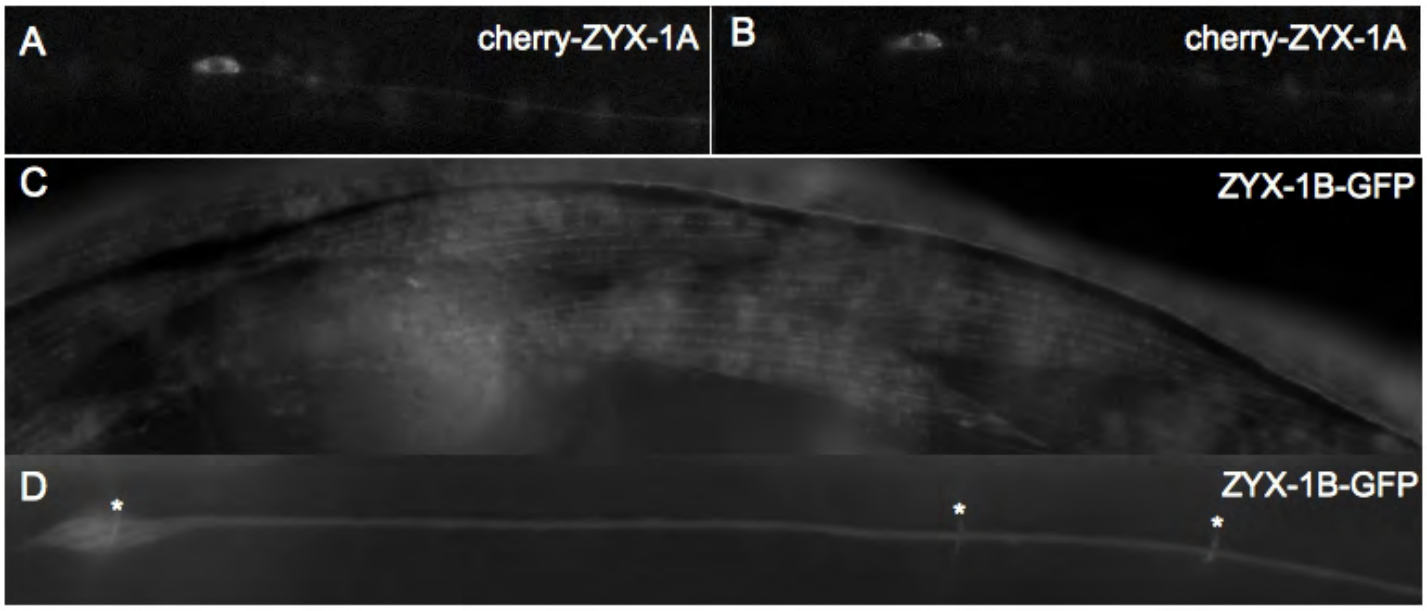

Figure S10. ZYX-1 subcellular localization
A, B) Two different focal planes demonstrating that fulllength functional mCherry-ZYX-1A fusion driven under the *mec-7* promoter, with the coding transgene integrated in single copy using MosSCI, was excluded from the nucleus in PLMs. Images of *jsIs1103* are shown. Scale bar, 10 µm.
C) ZYX-1B localizes in a punctate pattern resembling dense body localization in muscle. A ZYX-1B-GFP fusion driven under the *zyx-1* P3 promoter was expressed in muscle and localized largely to punctate structures which are likely muscle dense body adhesion sites. Images of *jsEx1291* are shown. Scale bar, 10 µm.
D) The *zyx-1* P3 promoter drove expression in TNRs and ZYX-1B-GFP fusion was largely ubiquitously localized in neuronal processes. The small vertical neurite structure crossing the soma and the distal portion of the ALM neurite were motor neuron commissures (*). Images of *jsEx1291* are shown. Scale bar, 10 µm.

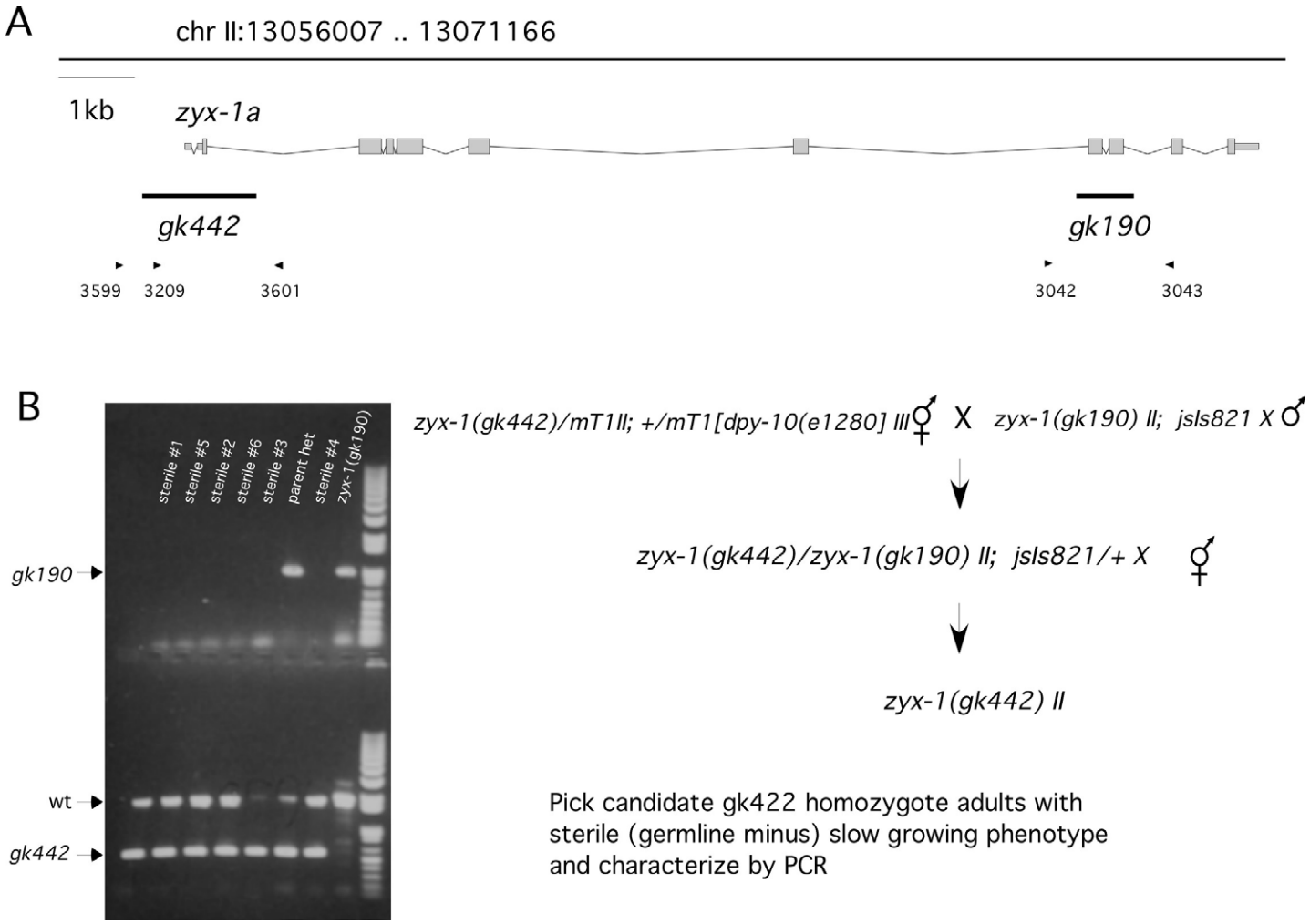

Figure S11. Analysis of the *gk442* deletion mutant
A) Structure of the *zyx-1* locus showing the position of the *gk190* and *gk442* deletions as defined by the *C. elegans* knockout consortium as well as the position of oligonucleotides used in B). Sequences of oligonucleotides are listed in Table S5.
B) On the right are the outlined cross strategy used to isolate putative *gk442* homozygote sterile animals. On the left are the results of PCR amplification from individual sterile animals. Note that most sterile animals lacked the *gk190* allele thus must be homozygous for the non-*gk190* allele. Despite this, they contained wild-type sequences when amplified for the *gk442* deletion, suggesting that the *gk442* locus is not a simple deletion and the deletion may not be linked to *zyx-1*.

Supplementary references

Godinho, L., Mumm, J. S., Williams, P. R., Schroeter, E. H., Koerber, A., Park, S. W., Leach, S. D. and Wong, R. O. (2005). Targeting of amacrine cell neurites to appropriate synaptic laminae in the developing zebrafish retina. *Development* **132**, 5069-79.
Larkin, M. A., Blackshields, G., Brown, N. P., Chenna, R., McGettigan, P. A., McWilliam, H., Valentin, F., Wallace, I. M., Wilm, A., Lopez, R. et al. (2007). Clustal W and Clustal X version 2.0. *Bioinformatics* **23**, 2947-8.
Mahoney, T. R., Liu, Q., Itoh, T., Luo, S., Hadwiger, G., Vincent, R., Wang, Z. W., Fukuda, M. and Nonet, M. L. (2006). Regulation of synaptic transmission by RAB-3 and RAB-27 in Caenorhabditis elegans. *Mol Biol Cell* **17**, 2617-25.
Mahoney, T. R., Luo, S., Round, E. K., Brauner, M., Gottschalk, A., Thomas, J. H. and Nonet, M. L. (2008). Intestinal signaling to GABAergic neurons regulates a rhythmic behavior in Caenorhabditis elegans. *Proc Natl Acad Sci U S A* **105**, 16350-5.
Matsuki, M., Kunitomo, H. and Iino, Y. (2006). Goalpha regulates olfactory adaptation by antagonizing Gqalpha-DAG signaling in Caenorhabditis elegans. *Proc Natl Acad Sci U S A* **103**, 1112-7.
Sarov, M., Schneider, S., Pozniakovski, A., Roguev, A., Ernst, S., Zhang, Y., Hyman, A. A. and Stewart, A. F. (2006). A recombineering pipeline for functional genomics applied to Caenorhabditis elegans. *Nat Methods* **3**, 839-44.
Shaner, N. C., Campbell, R. E., Steinbach, P. A., Giepmans, B. N., Palmer, A. E. and Tsien, R. Y. (2004). Improved monomeric red, orange and yellow fluorescent proteins derived from Discosoma sp. red fluorescent protein. *Nat Biotechnol* **22**, 1567-72.
Tseng, W. C., Lin, J. W., Wei, T. Y. and Fang, T. Y. (2008). A novel megaprimed and ligase-free, PCR-based, site-directed mutagenesis method. *Anal Biochem* **375**, 376-8.

Table S1. PLM synapse phenotype of focal adhesion complex mutants

			Synaptic varicosities[1]		
Genotype[2]	**Protein(s) affected**	**n**	**Two**	**One**	**None**
Wild type		103	98%	2%	0%
zyx-1(js417)[3]	zyxin focal adhesion protein	50	2.8%	17.2%	80.0%
zyx-1(gk190)[3]	zyxin focal adhesion protein	112	3.5%	17.9%	78.6%
	Focal Adhesion complex mutants				
kin-32(ok166)[3]	focal adhesion kinase	97	97%	3%	0%
zyx-1(gk190); kin-32(ox166)[3]	zyxin; focal adhesion kinase	155	5.2%	20.6%	73.5%
unc-97(su110)[4]	LIM domain PINCH family focal adhesion protein	40	100%	0%	0%
unc-98(su130)[4]	Zinc finger-containing muscle M-line protein	48	75%	23%	2%
ina-1(gm39)	α-integrin subunit	25	100%	0%	0%
ina-1(gm144)	α-integrin subunit	50	96%	2%	2%
pat-3;[pat-3(Y804F)]	β-integrin subunit; C-terminal tyrosine residue mutated	79	74.7%	17.7%	7.6%
pat-4;[pat-4(S334A)::GFP]	Integrin-linked kinase; no kinase activity	90	87.8%	7.8%	4.4%
hmp-1(pe97)	α-catenin	40	95%	5%	0%
bar-1(ga80[3]*)*	β-catenin	20	90%	10%	0%
pry-1(mu38)[3]	RGS domain-containing protein; negative regulator of beta-catenin and Wnt signaling	75	96%	4%	0%

Notes

1) scored at RT (~22.5°C). Scoring of synaptic varicosities described in methods. The frequency of synapses for *zyx-1* is lower than in Figure 2 because many of the small synapses (Figure S4 breakdown of Figure 2) were not scored as synapses in our bulk scoring assay.

2) all strains in *jsIs821* background unless noted.

3) contains *jsIs973;* duplicate of data presented in Table 1.

4) strong locomotion defect. Lack of phenotype could be result of suppression by lack of muscle contractions.

Table S2. Alleles used in this study

mutant allele	**reference**
alp-1(ok820)	(Han and Beckerle, 2009)
atn-1(ok84)	(Moulder et al., 2010)
bar-1(ga80)	(Eisenmann et al., 1998)
dlk-1(km12)	(Bounoutas et al., 2009)
dyc-1(cx32)	(Gieseler et al., 2000)
glh-1(gk100)	(Lall et al., 2005)
hmp-1(fe4)	(Pettitt et al., 2003)
ina-1(gm144)	(Baum and Garriga, 1997)
ina-1(gm39)	(Baum and Garriga, 1997)
kin-32(ok166)	(Cram et al., 2008)
lim-8(ok941)	(Qadota et al., 2007)
lim-9(gk106)	(Qadota et al., 2007)
mkk-4(ok1545)	(Bounoutas et al., 2009)
pat-3(st564)	(Poinat et al., 2002)
pat-4(st551)	(Mackinnon et al., 2002)
pmk-3(ok169)	(Nakata et al., 2005)
pry-1(mu38)	(Korswagen et al., 2002)
scpl-1(ok1080)	(Qadota et al., 2008)
syg-1(ky652)	(Shen and Bargmann, 2003)
syg-2(ky671)	(Shen et al., 2004)
uig-1(ok884)	(Hikita et al., 2005)
unc-15(e73)	(Deitiker and Epstein, 1993)
unc-34(e315)	(Fleming et al., 2010)
unc-54(e190)	(Waterston et al., 1982)
unc-97(su110)	(Hobert et al., 1999)
unc-98(su130)	(Mercer et al., 2003)
unc-112(r367)	(Rogalski et al., 2000)
zyx-1(gk190)	(Lecroisey et al., 2008)
zyx-1(js417)	this study

References

Baum, P. D. and Garriga, G. (1997). Neuronal migrations and axon fasciculation are disrupted in ina-1 integrin mutants. *Neuron* **19**, 51-62.

Bounoutas, A., Zheng, Q., Nonet, M. L. and Chalfie, M. (2009). mec-15 Encodes an F-box Protein Required for Touch Receptor Neuron Mechanosensation, Synapse Formation, and Development. *Genetics* **183**, 607-617.

Cram, E. J., Fontanez, K. M. and Schwarzbauer, J. E. (2008). Functional characterization of KIN-32, the Caenorhabditis elegans homolog of focal adhesion kinase. *Dev Dyn* **237**, 837-846.

Deitiker, P. R. and Epstein, H. F. (1993). Thick filament substructures in Caenorhabditis elegans: evidence for two populations of paramyosin. *J Cell Biol* **123**, 303-311.

Eisenmann, D. M., Maloof, J. N., Simske, J. S., Kenyon, C. and Kim, S. K. (1998). The beta-catenin homolog BAR-1 and LET-60 Ras coordinately regulate the Hox gene lin-39 during Caenorhabditis elegans vulval development. *Development* **125**, 3667-3680.

Fleming, T., Chien, S. C., Vanderzalm, P. J., Dell, M., Gavin, M. K., Forrester, W. C. and Garriga, G. (2010). The role of C. elegans Ena/VASP homolog UNC-34 in neuronal polarity and motility. *Dev Biol* **344**, 94-106.

Gieseler, K., Grisoni, K. and Segalat, L. (2000). Genetic suppression of phenotypes arising from mutations in dystrophin-related genes in Caenorhabditis elegans. *Curr Biol* **10**, 1092-1097.

Han, H. F. and Beckerle, M. C. (2009). The ALP-Enigma protein ALP-1 functions in actin filament organization to promote muscle structural integrity in Caenorhabditis elegans. *Mol Biol Cell* **20**, 2361-2370.

Hikita, T., Qadota, H., Tsuboi, D., Taya, S., Moerman, D. G. and Kaibuchi, K. (2005). Identification of a novel Cdc42 GEF that is localized to the PAT-3-mediated adhesive structure. *Biochem Biophys Res Commun* **335**, 139-145.
Hobert, O., Moerman, D. G., Clark, K. A., Beckerle, M. C. and Ruvkun, G. (1999). A conserved LIM protein that affects muscular adherens junction integrity and mechanosensory function in Caenorhabditis elegans. *J Cell Biol* **144**, 45-57.
Korswagen, H. C., Coudreuse, D. Y., Betist, M. C., van de Water, S., Zivkovic, D. and Clevers, H. C. (2002). The Axin-like protein PRY-1 is a negative regulator of a canonical Wnt pathway in C. elegans. *Genes Dev* **16**, 1291-1302.
Lall, S., Piano, F. and Davis, R. E. (2005). Caenorhabditis elegans decapping proteins: localization and functional analysis of Dcp1, Dcp2, and DcpS during embryogenesis. *Mol Biol Cell* **16**, 5880-5890.
Lecroisey, C., Martin, E., Mariol, M. C., Granger, L., Schwab, Y., Labouesse, M., Segalat, L. and Gieseler, K. (2008). DYC-1, a protein functionally linked to dystrophin in Caenorhabditis elegans is associated with the dense body, where it interacts with the muscle LIM domain protein ZYX-1. *Mol Biol Cell* **19**, 785-796.
Mackinnon, A. C., Qadota, H., Norman, K. R., Moerman, D. G. and Williams, B. D. (2002). C. elegans PAT-4/ILK functions as an adaptor protein within integrin adhesion complexes. *Curr Biol* **12**, 787-797.
Mercer, K. B., Flaherty, D. B., Miller, R. K., Qadota, H., Tinley, T. L., Moerman, D. G. and Benian, G. M. (2003). Caenorhabditis elegans UNC-98, a C2H2 Zn finger protein, is a novel partner of UNC-97/PINCH in muscle adhesion complexes. *Mol Biol Cell* **14**, 2492-2507.
Moulder, G. L., Cremona, G. H., Duerr, J., Stirman, J. N., Fields, S. D., Martin, W., Qadota, H., Benian, G. M., Lu, H. and Barstead, R. J. (2010). α-actinin is required for the proper assembly of Z-disk/focal-adhesion-like structures and for efficient locomotion in Caenorhabditis elegans. *J Mol Biol* **403**, 516-528.
Nakata, K., Abrams, B., Grill, B., Goncharov, A., Huang, X., Chisholm, A. D. and Jin, Y. (2005). Regulation of a DLK-1 and p38 MAP kinase pathway by the ubiquitin ligase RPM-1 is required for presynaptic development. *Cell* **120**, 407-420.
Pettitt, J., Cox, E. A., Broadbent, I. D., Flett, A. and Hardin, J. (2003). The Caenorhabditis elegans p120 catenin homologue, JAC-1, modulates cadherin-catenin function during epidermal morphogenesis. *J Cell Biol* **162**, 15-22.
Poinat, P., De Arcangelis, A., Sookhareea, S., Zhu, X., Hedgecock, E. M., Labouesse, M. and Georges-Labouesse, E. (2002). A conserved interaction between beta1 integrin/PAT-3 and Nck-interacting kinase/MIG-15 that mediates commissural axon navigation in C. elegans. *Curr Biol* **12**, 622-631.
Qadota, H., McGaha, L. A., Mercer, K. B., Stark, T. J., Ferrara, T. M. and Benian, G. M. (2008). A novel protein phosphatase is a binding partner for the protein kinase domains of UNC-89 (Obscurin) in Caenorhabditis elegans. *Mol Biol Cell* **19**, 2424-2432.
Qadota, H., Mercer, K. B., Miller, R. K., Kaibuchi, K. and Benian, G. M. (2007). Two LIM domain proteins and UNC-96 link UNC-97/pinch to myosin thick filaments in Caenorhabditis elegans muscle. *Mol Biol Cell* **18**, 4317-4326.
Rogalski, T. M., Mullen, G. P., Gilbert, M. M., Williams, B. D. and Moerman, D. G. (2000). The UNC-112 gene in Caenorhabditis elegans encodes a novel component of cell-matrix adhesion structures required for integrin localization in the muscle cell membrane. *J Cell Biol* **150**, 253-264.
Shen, K., Fetter, R. D. and Bargmann, C. I. (2004). Synaptic specificity is generated by the synaptic guidepost protein SYG-2 and its receptor, SYG-1. *Cell* **116**, 869-881.
Shen, K. and Bargmann, C. I. (2003). The immunoglobulin superfamily protein SYG-1 determines the location of specific synapses in C. elegans. *Cell* **112**, 619-630.
Waterston, R. H., Smith, K. C. and Moerman, D. G. (1982). Genetic fine structure analysis of the myosin heavy chain gene unc-54 of Caenorhabditis elegans. *J Mol Biol* **158**, 1-15.

Table S3. Trangenic markers

Transgenic marker	**Reference**	***Equivalent markers***
jsEx448 [Pmec-7::UNC-10::GFP; pJM23(lin-15)]	this study	*jsEx449*, *jsEx450*
jsIs608 [Pmec7::mito-GFP; pJM23(lin-15)]	this study	*jsIs609*
jsIs821 [Pmec-7::GFP::rab-3 CBunc-119]	(Bounoutas et al., 2009)	
jsEx968 [WRM0617bB03 (*zyx-1*); WRM062bF09 (*lin-15*)]	this study	
jsIs973 [Pmec-7::mRFP CBunc-119]	(Zheng et al., 2011)	
jsEx985 [NM1798 (pZ*yx-1*gen); pPD118.33 (*myo-2::GFP*)]	this study	*jsEx986*
jsEx1013 [NM1860 (*mcherry::zyx-1*); NM1874 (*zyx-1::GFP*), 1:1]	this study	*jsEx1014*
jsEx1015 [NM1934(P*mec-7::zyx-1(fl)::GFP*) ; pPD118.33 (*myo-2::GFP*)]	this study	*jsEx1017*
jsEx1020 [NM1938(P*glr-1::zyx-1(fl)::GFP*) ; pPD118.33 (P*myo-2::GFP*)]	this study	*jsEx1021*
jsEx1024 [NM1941(P*myo-3::zyx-1(fl)::YFP*); pPD118.33 (P*myo-2::GFP*)]	this study	*jsEx1025*
jsEx1037 [NM2008(P*mec-7::GFP::zyx-1(a.a.428-603)*, pPD118.33(P*myo-2::GFP*)]	this study	*jsEx1038*
jsEx1043 [NM2004(P*mec-7::GFP::zyx-1(a.a.1-293)*) ; pPD118.33 (P*myo-2::GFP*)]	this study	*jsEx1044*
jsEx1045 [NM2002(P*mec-7::GFP::zyx-1(a.a.1-427)* ; pPD118.33(P*myo-2::GFP*)]	this study	*jsEx1046*
jsEx1047 [NM2006(P*mec-7::GFP::zyx-1(a.a.294-603)*); pPD118.33(P*myo-2::GFP*)]	this study	j*sEx1048*
jsIs1103 [NM2122 (Pmec-7::cherry-zyx-1-GFP CBunc-119)]	this study	*jsIs1102*
jsEx1216 [NM2395 (P1xyz-1::nlsYFP]	this study	*jsEx1217*

jsEx1218 [NM2397 (P2*zyx-1::nlsYFP*)]	this study	*jsEx1219, jsEx1220*
jsEx1221 [NM2399 (P3*zyx-1::nlsYFP*)]	this study	*jsEx1222*
jsEx1223 [NM2387 (Pmec-7::Venus::LIM1); pPD118.33 (Pmyo-2::GFP)]	this study	*jsEx1224*
jsEx1225 [NM2389 (Pmec-7::Venus::LIM2); pPD118.33 (Pmyo-2::GFP)]	this study	
jsEx1226 [NM2390 (Pmec-7::Venus::LIM3); pPD118.33 (Pmyo-2::GFP)]	this study	*jsEx1227*
jsEx1228 [NM2391 (Pmec-7::Venus::LIM1,2); pPD118.33 (Pmyo-2::GFP)]	this study	*jsEx1229*
jsEx1232 [NM2392 (Pmec-7::Venus::LIM2,3); pPD118.33 (Pmyo-2::GFP)]	this study	*jsEx1234*
jsEx1233 [NM2394 (Pmec-7::Venus::LIM1,3); pPD118.33 (Pmyo-2::GFP)]	this study	
jsEx1287 [NM2911 Pmec-7;::zyx-1B::GFP; pPD132.102(Pmyo-2::GFP)]	this study	
jsEx1290 [NM2909 (ΔP12 zyx-1B); pPD132.102(Pmyo2:nlsYFP)]	this study	
jsEx1291 [NM2918 (ΔP12 zyx-1B-GFP); pCFJ90(Pmyo-2::mCherry)]	this study	
jsEx1388 [NM3099 (eGFP-zyx-1B); pcDNA3]	this study	*jsEx1389*
jsEx1389 [NM3100 (eGFP-zyx-1B); pcDNA3]	this study	*jsEx1388*
geIn3[sir-2.1;pRF4]	(Tissenbaum and Guarente, 2001)	
mdIs135[P*unc-17::GFP*]	(Mahoney et al., 2008)	
mwEx31 [pat-3(Y804F),sur-5::gfp]	(Lee et al., 2001)	
nuIs25[*glr-1::GFP*]	(Rongo et al., 1998)	
oxIs12[P*unc-47::GFP*]	(Knobel et al., 2001)	

zpEx225[GFP::pat-4(S334A);rol-6]	(Mackinnon et al., 2002)	

Bounoutas, A., Zheng, Q., Nonet, M. L. and Chalfie, M. (2009). mec-15 Encodes an F-box Protein Required for Touch Receptor Neuron Mechanosensation, Synapse Formation, and Development. *Genetics* **183**, 607-17.
Knobel, K. M., Davis, W. S., Jorgensen, E. M. and Bastiani, M. J. (2001). UNC-119 suppresses axon branching in C. elegans. *Development* **128**, 4079-92.
Lee, M., Cram, E. J., Shen, B. and Schwarzbauer, J. E. (2001). Roles for beta(pat-3) integrins in development and function of Caenorhabditis elegans muscles and gonads. *J Biol Chem* **276**, 36404-10.
Mackinnon, A. C., Qadota, H., Norman, K. R., Moerman, D. G. and Williams, B. D. (2002). C. elegans PAT-4/ILK functions as an adaptor protein within integrin adhesion complexes. *Curr Biol* **12**, 787-97.
Mahoney, T. R., Luo, S., Round, E. K., Brauner, M., Gottschalk, A., Thomas, J. H. and Nonet, M. L. (2008). Intestinal signaling to GABAergic neurons regulates a rhythmic behavior in Caenorhabditis elegans. *Proc Natl Acad Sci U S A* **105**, 16350-5.
Rongo, C., Whitfield, C. W., Rodal, A., Kim, S. K. and Kaplan, J. M. (1998). LIN-10 is a shared component of the polarized protein localization pathways in neurons and epithelia. *Cell* **94**, 751-759.
Zheng, Q., Schaefer, A. M. and Nonet, M. L. (2011). Regulation of C. elegans presynaptic differentiation and neurite branching via a novel signaling pathway initiated by SAM-10. *Development* **138**, 87-96.

Table S4. Strains

Strain	Genotype	Source
NM2689	*jsIs821 [Pmec-7::GFP::RAB-3 Cbunc-119]*	(Bounoutas et al., 2009)
NM3336	*jsIs973 [Pmec-7::mRFP, Cbunc-119]*	(Zheng et al., 2011)
NM2296	*jsIs608 [Pmec7::mtGFP; pJM23(lin-15)]*	This study
NM1731	*jsEx448 [Pmec-7::unc-10::GFP ;pJM23(lin-15)];lin-15(n765)]*	This study
NM3751	*unc-119(ed3); jsIs1103 [NM2122(Pmec-7cherryZyxgfpCbunc-119)]*	This study
NM3361	*jsIs973; jsIs821*	(Zheng et al., 2011)
NM3386	*jsIs608; jsIs973*	This study
	jsEx448; jsIs973	This study
NM3321	*zyx-1(js417); lin-15(n765) jsIs821; jsEx968* [WRM0617bB03 (*zyx-1*); WRM062bF09 (*lin-15*)]	This study
NM3425	*jsEx1013* [NM1860 (*mcherry::zyx-1*); NM1874 (*zyx-1::GFP*), 1:1]	This study
NM3434	*zyx-1(js417)*; *jsEx1015* [NM1934(P*mec-7::zyx-1(full length)::GFP*) ; pPD118.33 (*myo-2::GFP*)]	This study
NM3439	*zyx-1(js417)*; *jsEx1020* [NM1938(P*glr-1::zyx-1(full length)::GFP*) ; pPD118.33 (P*myo-2::GFP*)]	This study
NM3443	*zyx-1(js417)*; *jsEx1024* [NM1941 (P*myo-3::zyx-1(full length)::YFP*); pPD118.33 (P*myo-2::GFP*)]	This study
NM3473	*zyx-1(js417)*; *jsEx1037* [NM2008 (P*mec-7::GFP::zyx-1(a.a. 428-603)*, pPD118.33(P*myo-2::GFP*)]	This study
NM3424	*zyx-1(js417)*; *jsEx1043* [NM2004 (P*mec-7::GFP::zyx-1(a.a. 1-293)*) ; pPD118.33 (P*myo-2::GFP*)]	This study
NM3481	*zyx-1(js417)*; *jsEx1045* [NM2002 (P*mec-7::GFP::zyx-1(a.a. 1-427)* ; pPD118.33(P*myo-2::GFP*)]	This study
NM3483	*zyx-1(js417)*; *jsEx1047* [NM2006 (P*mec-7::GFP::zyx-1(a.a. 294-603)*); pPD118.33(P*myo-2::GFP*)]	This study
NM3751	*jsIs1103 [NM2122 (Pmec-7::cherry-zyx-1-GFP CBunc-119)]*	This study
NM4031	*jsEx1216 [NM2395 (P1zyx-1::nlsYFP]*	This study
NM4033	*jsEx1218 [NM2397 (P2zyx-1::nlsYFP)]*	This study
NM4036	*jsEx1221 [NM2399 (P3zyx-1::nlsYFP)]*	This study
NM4038	*zyx-1(gk190); jsIs973; jsIs821*; *jsEx1223 [NM2387 (Pmec-7::Venus::LIM1); pPD118.33 (Pmyo-2::GFP)]*	This study
NM4040	*zyx-1(gk190); jsIs973; jsIs821*; *jsEx1225 [NM2389 (Pmec-7::Venus::LIM2); pPD118.33 (Pmyo-2::GFP)]*	This study
NM4041	*zyx-1(gk190); jsIs973; jsIs821*; *jsEx1226 [NM2390 (Pmec-7::Venus::LIM3); pPD118.33 (Pmyo-2::GFP)]*	This study

NM4043	*zyx-1(gk190); jsIs973; jsIs821*; *jsEx1228 [NM2391 (Pmec-7::Venus::LIM1,2); pPD118.33 (Pmyo-2::GFP)]*	This study
NM4047	*zyx-1(gk190); jsIs973; jsIs821*; *jsEx1232 [NM2392 (Pmec-7::Venus::LIM2,3); pPD118.33 (Pmyo-2::GFP)]*	This study
NM4048	*zyx-1(gk190); jsIs973; jsIs821*; *jsEx1233 [NM2394 (Pmec-7::Venus::LIM1,3); pPD118.33 (Pmyo-2::GFP)]*	This study
NM4429	*zyx-1(gk190); jsIs973; jsIs821*; *jsEx1287 [NM2911 Pmec-7;:zyx-1B::GFP; pPD132.102(Pmyo-2::GFP)]*	This study
NM4435	*zyx-1(gk190); jsIs973; jsIs821*; *jsEx1290 [NM2909 (ΔP12 zyx-1B); pPD132.102(Pmyo2:nlsYFP)]*	This study
NM4438	*zyx-1(gk190); jsIs973; jsIs821*; *jsEx1291 [NM2918 (ΔP12 zyx-1B-GFP); pCFJ90(Pmyo-2::mCherry)]*	This study
NM4659	*jsEx1388 [NM3099 (eGFP-zyx-1B); pcDNA3]*	This study
NM4660	*jsEx1389 [NM3100 (eGFP-zyx-1B); pcDNA3]*	This study
NM3410	*zyx-1(js417); jsIs821; jsIs973*	This study
VC299	*zyx-1(gk190)*	CGC
NM3414	*zyx-1(js417); jsIs608; jsIs973*	This study
NM3419	*zyx-1(js417); jsEx448; jsIs973*	This study
NM3413	*zyx-1(gk190); jsIs821; jsIs973*	This study
NM3416	*zyx-1(gk190); jsIs608; jsIs973*	This study
NM2874	*zyx-1(js417); jsIs821*	This study
NM4088	*zyx-1(gk190); jsIs1103; jsIs821*	This study
CX652	*kyIs235 [odr-1::RFP + unc-86::VAMP-YFP + unc-4::lin-10-RFP intron]; syg-1(ky652)*	CGC
NM2976	*syg-1(ky652) jsIs821*	This study
CX6391	*syg-2(ky671); kyEx648 [unc-86 p+ syg-1::GFP}*	CGC
NM2977	*jsIs821 syg-2(ky671)*	This study
NG144	*ina-1(gm144)*	CGC
NM3744	*ina-1(gm144); jsIs821*	This study
NG39	*ina-1(gm39)*	CGC
NM3713	*ina-1(gm39); jsIs821*	This study
JE31	*pat-3(st564); mwEx31[pat-3(Y804F), sur-5::GFP]*	Jean Schwarzbauer, Princeton U.
NM3702	*pat-3(st564); jsIs973;mwEx31*	This study
WB204	*pat-4(st551)III; zpEx225[GFP::PAT-4(S334A); rol-6]*	Ben Williams, U. of Illinois
NM3704	*pat-4(st551); jsIs821; zpEx225*	This study
CB73	*unc-15(e73)*	CGC
NM4131	*unc-15(e73); zyx-1(gk190); jsIs821*	This study
RW3024	*unc-54(e190)/let-50(st33)*	CGC
NM4122	*unc-54(e190); jsIs973; jsIs821*	This study
NM4123	*unc-54(e190); zyx-1(gk190); jsIs973; jsIs821*	This study
DV2208	*unc-97 (su110)*	CGC
NM3592	*unc-97(su110); jsIs821*	This study

HE130	*unc-98(su130)*	CGC
NM3712	*jsIs973; unc-98(su130)*	This study
VC1089	*mkk-4(ok1545)*	CGC
NM3215	*mkk-4(ok1545); jsIs821*	(Bounoutas et al., 2009)
NM3533	*zyx-1(gk190); mkk-4(ok1545); jsIs821*	This study
BS3383	*pmk-3(ok169)*	CGC
NM3211	*pmk-3(ok169); jsIs821*	(Bounoutas et al., 2009)
NM3552	*zyx-1(gk190); pmk-3(ok169); jsIs821*	This study
KU12	*dlk-1(km12)*	CGC
NM4481	*dlk-1(km12); jsIs973; jsIs821*	This study
NM4638	*zyx-1(gk190); dlk-1(km12); jsIs821*	This study
RB1812	*atn-1(ok84)*	CGC
NM3882	*atn-1(ok84); jsIs973; jsIs821*	This study
PE97	*hmp-1(fe4)*	*CGC*
NM4015	*hmp-1(fe4); jsIs821*	This study
EW15	*bar-1(ga80)*	*CGC*
NM4082	*jsIs973; bar-1(ga80) jsIs821*	This study
CF491	*pry-1(mu38); him-5(e1490)*	*CGC*
NM4058	*pry-1(mu38); jsIs821*	This study
RB776	*kin-32(ok166)*	*CGC*
NM4441	*kin-32(ok166); jsIs973; jsIs821*	This study
NM4464	*kin-32(ok166); zyx-1(gk190); jsIs973; jsIs821*	This study
LS396	*dyc-1(cx32)*	*CGC*
NM4442	*jsIs973; dyc-1(cx32) jsIs821*	This study
RB978	*uig-1(ok884)*	*CGC*
NM4612	*jsIs973; uig-1(ok884); jsIs821*	This study
VC179	*glh-1(gk100)*	*CGC*
NM4631	*glh-1(gk100); jsIs973; jsIs821*	This study
VC654	*lim-8(ok941)*	*CGC*
NM3454	*lim-8(ok941); jsIs821*	(Zheng et al., 2011)
VC209	*lim-9(gk106)*	*CGC*
NM3455	*lim-9(gk106); jsIs821*	(Zheng et al., 2011)
RB937	*alp-1(ok820)*	*CGC*
NM4612	*jsIs973; alp-1(ok820); jsIs821*	This study
RB1101	*scpl-1(ok1080)*	*CGC*
NM4623	*scpl-1(ok1080); jsIs973; jsIs821*	This study
DM5113	*unc-112(r367); raEx11 [pRF4(rol-6(su1006)) + pDM#208(unc-112(+))]*	*CGC*
NM4646	*zyx-1(gk190); jsIs973; unc-112(r367); jsIs821*	This study
NM4647	*jsIs973; unc-112(r367); jsIs821*	This study

References

Bounoutas, A., Zheng, Q., Nonet, M. L. and Chalfie, M. (2009). mec-15 Encodes an F-box Protein Required for Touch Receptor Neuron Mechanosensation, Synapse Formation, and Development. *Genetics* **183**, 607-617.

Zheng, Q., Schaefer, A. M. and Nonet, M. L. (2011). Regulation of C. elegans presynaptic differentiation and neurite branching via a novel signaling pathway initiated by SAM-10. *Development* **138**, 87-96.

Table S5. Oligonucleotides used in this study

Primer Name	Sequence	Use
1265	5’ TCGGGTCTCTCCAAAAACTC	scoring pkP2111 SNP
1266	5’ CTCCTTCAGTACCATATGGCTC	scoring pkP2111 SNP
1267	5’ TTCCCATTTTCCTCCCAG	scoring pkP2116 SNP
1268	5’ TCAAAAACCCAGACACTGG	scoring pkP2116 SNP
2778	5’ CCAGCTGCAGCAGCTTCATCTAC	scoring haw31582 SNP
2779	5’ ATTGCAAATTCACAGAACTCAGC	scoring haw31582 SNP
2820	5’ AATTTCGAACGCTCCAATGA	scoring CE2-207 SNP
2821	5’ CCTGAAGACATCCGGAAAAA	scoring CE2-207 SNP
2845	5’ GTATGTAAGGACACGAACGCAA	scoring pkP2112 SNP
2846	5’ GATAATTGAGATTTAAGCTGTG	scoring pkP2112 SNP
3007	5’ ACTGCCGCCACCATTGTTGAT	scoring Y38A1 [10] SNP
3008	5’ TAAACATTGAAGACTGCACAA	scoring Y38A1 [10] SNP
3009	5’ ACCGAATGTGATGTCCTAGAA	scoring F42G4[1] SNP
3010	5’ GATGTGGCCTAGAAAACAGAT	scoring F42G4[1] SNP
3011	5’ CCTCCAGTTTCCCAACTATCT	scoring F42G4[5] SNP
3012	5’ ACAACGGTGGGCACATAGCAT	scoring F42G4[5] SNP
3015	5’ CTCAGAAGTCATACTCGACAT	scoring uCE2-2180 SNP
3016	5’ ATTCGATTGGACCGAATGCTG	scoring uCE2-2180 SNP
3042	5’ CGGTAGCAGGATGGTTTTTG	scoring the *gk190* deletion
3043	5’ CCGACTCCTTTTCTCCGTCT	scoring the *gk190* deletion
3184	5’ AAATAAAAAAATAGAAAAATACTTGAAAAATATTGAAAAAGATTTTAAAA ATACAATTCGTTATGCATTATGGGTAC	constructing NM1798
3185	5’ TACAAATTCGGCAAATCGACAACTTGCCGGTTTGCCGGAAACTATCAATTTA CCAATCTAAGTCTGTGCTCC	constructing NM1798
3189	5’ CTGGAAATTTGGATTTACAATTATTT	scoring the *gk190* deletion
3209	5’ CACGCTGTGAACTCTAGGTTTT	scoring the *gk442* deletion
3265	TGAGACGAATTCCCGCTACCTCCTGAGCTAAG	constructing NM1849
3266	TGAGACGAATTCTGAAGTTCCTATTCTCTAGAAAG	constructing NM1849
3271	CCTCGCCCTTGCTCACCATGTCAGGAAGTTCCTATACTTTC	constructing NM1849
3272	GAAAGTATAGGAACTTCCTGACATGGTGAGCAAGGGCGAGG	constructing NM1849
3273	TCGCACCGGCAGATCGTCATTACTTGTACAGCTCGTCCATG	constructing NM1849
3274	CATGGACGAGCTGTACAAGTAATGACGATCTGCCGGTGCGA	constructing NM1849
3275	5’ CGTGCTCGCTCCTTCAGCACTATTCCAGACTCGGCATCCGCTACTGATCTGA ATTCTGAAGTTCCTATTCTCT	constructing NM1860
3277	5’ CTTACGGATGGGAGTAGAGGGGGTGGTGGAGGCGGAGGCGGGGGTCCCATC TTGTACAGCTCGTCCATGC	constructing NM1860
3278	5’ TGCTCTGCAAGACCTGTAATGGAAACCGGCTCCGCGTGGTCAGCTCCACGA GCTCAGGAGGTAGCGGCA	constructing NM1874
3279	5’ GAAGAAAAACGGATGGGGGGAATGGAAATTGTTGACTGATGGCTCGCTTAA CCGGCAGATCGTCAGTCAG	constructing NM1874
3362	5’ TGACACGTGGATCCATGGGACCCCCGCCTCCG	constructing NM1934, NM1938
3363	5’ TGACACGTCGGTACCAACGTGGAGCTGACCACGCGG	constructing NM1934
3364	5’ TGACACGTACTAGTCGTGGAGCTGACCACGCGG	constructing NM1938
3365	5’ TGACACGTGCTAGCATGGGACCCCCGCCTCCG	constructing NM1941
3366	5’ TGACACGTAGGCCTCGTGGAGCTGACCACGCGG	constructing NM1941
3384	5’ AGTGAGTTCTGATAGCAGCCTT	constructing NM2911
3406	5’ TGACACGTGGTACCATGAGTAAAGGAGAAGAACTTTTC	constructing NM2002, NM2004, NM2006, NM2008, NM2387 NM2389, NM2390, NM2391, NM2392, NM2394
3407	5’ CGGAGGCGGGGGTCCCATCTTGTATGGCCGGCTAGCGA	constructing NM2002, NM2004
3408	5’ TCGCTAGCCGGCCATACAAGATGGGACCCCCGCCTCCG	constructing NM2002,

		NM2004
3409	5’ TGACACGTGATATCTTATGCATTGCATCCTGGCTGGT	constructing NM2002
3410	5’ TGACACGTGATATCTTATCGTTGATAAAGATCTGGTGGT	constructing NM2004
3411	5’ GGAAAGTTCTTGCTTGAGTCATCTTGTATGGCCGGCTAGCGA	constructing NM2006
3412	5’ TCGCTAGCCGGCCATACAAGATGACTCAAGCAAGAACTTTCC	constructing NM2006
3413	5’ TGACACGTGATATCTTACGTGGAGCTGACCACGC	constructing NM2006, NM2008, NM2390, NM2392
3414	5’ CCACGTGGAAGATCTGATTCATCTTGTATGGCCGGCTAGCGA	constructing NM2008
3415	5’ TCGCTAGCCGGCCATACAAGATGAATCAGATCTTCCACGTGG	constructing NM2008
3419	5’ TGACACGTGGATCCATGGTGAGCAAGGGCGAGGA	constructing NM2016
3420	5’ CGGAGGCGGGGGTCCCATCTTGTACAGCTCGTCCATGC	constructing NM2016
3421	5’ GCATGGACGAGCTGTACAAGATGGGACCCCCGCCTCCG	constructing NM2016
3363	5’ TGACACGTCGGTACCAACGTGGAGCTGACCACGCGG	constructing NM2016
3599	5’ CCCACTTGAAAATATGACGTCACA	scoring the *gk442* deletion
3601	5’ TGACGTCACTCAGTTGCGCGGGAA	scoring the *gk442* deletion
4126	5’ TCTACGATGCTAGCGAGGTGGAACGTGCGACATT	constructing NM2395
4127	5’ GCTTCTTCTTTGGAGCAGTCATGAGCTCCTAGAAGTTAATTTCTTACTTTTGG	constructing NM2395
4128	5’ CCAAAAGTAAGAAATTAACTTCTAGGAGCTCATGACTGCTCCAAAGAAGAAGC	constructing NM2395
4129	5’ TCTACGATCTCGAGCTATTTGTATAGTTCATCCATGC	constructing NM2395, NM2397, NM2399
4130	TCTACGATCTCGAGCGCGGATAACAAATTTCATATGTT	constructing NM2399
4131	TCTACGATGCTAGCGGGCTGCAGGTTTTTGTTCTG	constructing NM2399
4132	5’ TCTACGATGCTAGCGTTAGTTGTCATCGTCGTAGTTT	constructing NM2397
4133	5’ GCTTCTTCTTTGGAGCAGTCATGAGCTCCTGGAAATATGTGTTTTAAGGAAT	constructing NM2397
4134	5’ ATTCCTTAAAACACATATTTCCAGGAGCTCATGACTGCTCCAAAGAAGAAGC	constructing NM2397
4135	5’ TCTACGATGCTAGCGTGGGTTTTTCTTCTTTTTCTTTT	constructing NM2399
4136	5’ GCTTCTTCTTTGGAGCAGTCATGAGCTCTGCATTGCATCCTGGCTGGT	constructing NM2399
4137	5’ ACCAGCCAGGATGCAATGCAGAGCTCATGACTGCTCCAAAGAAGAAGC	constructing NM2399
4138	5’ CCAACGCAGATATTGATATTCATGGATCCTTTGTATAGTTCATCCATGCCAA	constructing NM2387, NM2391, NM2394
4139	5’ TTGGCATGGATGAACTATACAAAGGATCCATGAATATCAATATCTGCGTTGG	constructing NM2387, NM2391, NM2394
4140	5’ TGACACGTGATATCTTATGAGTTCTGATAGCAGCCTTC	constructing NM2387
4141	5’ CACGCGGTACACTTCTCCAGGGATCCTTTGTATAGTTCATCCATGCCAA	constructing NM2389, NM2392
4142	5’ TTGGCATGGATGAACTATACAAAGGATCCCTGGAGAAGTGTACCGCGTG	constructing NM2389, NM2392
4143	5’ TGACACGTGATATCTTATTTGTCATGGAAGCATGGGACA	constructing NM2389, NM2391, NM2394
4144	5’ AGTGCACATCGTGGCGCGAAGGATCCTTTGTATAGTTCATCCATGCCAA	constructing NM2390
4145	5’ TTGGCATGGATGAACTATACAAAGGATCCTTCGCGCCACGATGTGCACT	constructing NM2390
4146	5’ AGTGCACATCGTGGCGCGAATGAGTTCTGATAGCAGCCTTC	constructing NM2394
4147	5’ GAAGGCTGCTATCAGAACTCATTCGCGCCACGATGTGCACT	constructing NM2394
4852	5’ CTAGCCGGCCATACAAGATGGCGGATCAAGAAGATATCTGCGTTGGTTGTGGC	constructing NM2911
5157	5’ TTACTACATATTCTCTGTTTTTTTTCTGGGTTCTGAACTTGTTTTGAACTGAAT TCTGAAGTTCCTATTCTCT	constructing NM3099,NM3100
5218	5’AACACAAATTTTCAGCTTCGAAAAAAAAACGAACCTTCTTGATCCGCCAT TCCGCGGCCGTCCTTGTAC	constructing NM3099, NM3100
2766	5’ TTCAGAGTTAATGGTTCAAGAAG	scoring *mkk-4(ok1545)*
2767	5’ AAATGTCCATCAGTTCCATGC	scoring *mkk-4(ok1545)*
2768	5’ ACTCACTGTAGCAATCTGATC	scoring *mkk-4(ok1545)*
2769	5’ CTTCTCAAAAAATGAGCTATGCG	scoring *pmk-3(ok169)*
2770	5’ TTCACTTCAAGCCCTAACTTG	scoring *pmk-3(ok169)*
2771	5’ CTTTGTATGTCTTCCTCTCGT	scoring *pmk-3(ok169)*
3546	5’ AACACTGCTGGAAACAAGACAG	scoring *lim-9(gk106)*
3547	5’ TTGGCTAGTCATTGATGGGCTC	scoring *lim-9(gk106)*
3550	5’ ATGCCTGAGGTATCTGTTGAG	scoring *lim-8(ok941)*
3551	5’ GTGTCTCTCTTGTCTTCTACGG	scoring *lim-8(ok941)*

3737	5’ AGATGCCATTGACACCTTCC	scoring *atn-1(ok84)*
3738	5’ CGTCCGGTACAGACAGAATA	scoring *atn-1(ok84)*
3739	5’ ATTCACAGCCTGGTGCAACT	scoring *atn-1(ok84)*
3740	5’ CCGACACGAAGCGATTCCAT	scoring *atn-1(ok84)*
4115	5’ CATCCATGGCCGACTATGAGCCGATCCCCACTGATTCAGAT	scoring *bar-1(ga80)*
4116	5’ TCTTACATTATCCTGATCTTTC	scoring *bar-1(ga80)*
4863	5’ AGGAAGCATACCCGGCATTTG	scoring *dyc-1(cx32)*
4864	5’ CGTTACCTTCCTTATCTGAGAATCCCG	scoring *dyc-1(cx32)*
4865	5’ GCAGCGTGTTATCCATGTCGTC	scoring *kin-32(ok166)*
4866	5’ CCGCCACAGCTATCCGTTCATC	scoring *kin-32(ok166)*
4867	5’ ATCAATCATCCGAAGCTTGGCAC	scoring *kin-32(ok166)*
4931	5’ CCACAGGGATCTCAAATCGCCC	scoring *dlk-1(km12)*
4932	5’ CCAGGACATCCGAAATATGTACGAG	scoring *dlk-1(km12)*
4933	5’ GGCGGATTCGCTCCCTCGC	scoring *dlk-1(km12)*
5166	5’ CCATCTACAACACACCCAGAAGAATTG	scoring *uig-1(ok884)*
5167	5’ CACGCCTATTGTTCCTGTTTGAGG	scoring *uig-1(ok884)*
5168	5’ AGTAGTTAGGATCAGTTGATTGGGTTGG	scoring *uig-1(ok884)*
5184	5’ ACAACAATTCTGCTGGTAACCGTG	scoring *uig-1(ok884)*
5201	5’ CCGATAAGTCTGCAGCTGAGC	scoring *alp-1(ok820)*
5202	5’ GCTGCACGAGCCATCACTC	scoring *alp-1(ok820)*
5203	5’ AACCTCACTGCAGCTTTCAGAG	scoring *alp-1(ok820)*
5207	5’ ACATGGCGGCGGAGAGAG	scoring *glh-1(gk100)*
5208	5’ GCTTGATGGTACCCTCTTCACAG	scoring *glh-1(gk100)*
5209	5’ CGGAAGCTAATCTCACGGAGACC	scoring *glh-1(gk100)*
5213	5’ GAAACGGGTATTCAGAGGACGAC	scoring *scpl-1(ok1080)*
5214	5’ GGAACGAAGGCACTGGATGG	scoring *scpl-1(ok1080)*
5215	5’ ACCACGTCGTCACTGGTACC	scoring *scpl-1(ok1080)*

Table S6. Mapping Single Nucleotide Polymorphisms

SNP	Position	Digest	Primer 1[a]	Primer 2[a]
pkP2111	II:12,323,043	EcoRI	NM1265	NM1266
haw31582	II:12773,543	TaqI	NM2778	NM2779
pkP2112	II:12,990,834	AciI	NM2845	NM2846
Y38A1[10]	II:13,004,876	MseI	NM3007	NM3008
F42G4[1]	II:13,056.066	HpyCH4V	NM3009	NM3010
F42G4[5]	II:13,067,284	sequenced	NM3011	NM3012
uCE2-2180	II:13,155,448	EcoRI	NM3015	NM3016
CE2-207	II:13,178,740	DraI	NM2820	NM2821
pKP2116	II:13,235,598	DraI	NM1267	NM1268

[a] Primer sequences in Table S5.